TABIMPUTE: ACCURATE AND FAST ZERO-SHOT MISSING-DATA IMPUTATION WITH A PRE-TRAINED TRANSFORMER

Anonymous authors
Paper under double-blind review

ABSTRACT

Missing data is a pervasive problem in tabular settings. Existing solutions range from simple averaging to complex generative adversarial networks, but due to each method's large variance in performance across real-world domains and time-consuming hyperparameter tuning, no default imputation method exists. Building on TabPFN, a recent tabular foundation model for supervised learning, we propose TabImpute, a pre-trained transformer that delivers accurate and fast zero-shot imputations requiring no fitting or hyperparameter tuning at inference-time. To train and evaluate TabImpute, we introduce (i) an entry-wise featurization for tabular settings, which enables a $100\times$ speedup over the previous TabPFN imputation method, (ii) a synthetic training data generation pipeline incorporating realistic missingness patterns, and (iii) MissBench, a comprehensive benchmark with 42 OpenML datasets and 13 new missingness patterns. MissBench spans domains such as medicine, finance, and engineering, showcasing TabImpute's robust performance compared to 12 established imputation methods.

1 INTRODUCTION

Missing data is ubiquitous across tabular datasets, affecting statisticians, economists, health officials, and businesses. For example, healthcare datasets may lack some recorded blood pressure measurements, or datasets merged from multiple sources may only share partial features. Regardless of the source, missing data must be imputed to numerical values before employing statistical or machine learning models. Imputation methods range from simple approaches (e.g., constant values and averages) to more sophisticated techniques like nearest-neighbor-based methods (Batista & Monard, 2003), matrix factorization approaches such as SoftImpute (Hastie et al., 2015), and random forest regression, notably the MissForest algorithm (Stekhoven & Bühlmann, 2011). However, each method in the literature is typically tailored for specific settings, with performance varying significantly across datasets, domains, and missingness patterns (Van Buuren, 2012; Jarrett et al., 2022; Agarwal et al., 2023; Ibrahim et al., 2005). Building on recent advances in tabular representation learning (Hollmann et al., 2023; Ye et al., 2025), we propose a pre-trained transformer specifically designed for the tabular missing-data problem that produces accurate and fast zero-shot imputations.

Rubin (1976) proposed analyzing missingness based on its relationship with the data-generating process to determine whether missingness biases downstream estimation. Rubin demonstrated that when missingness operates independently of the underlying data, the observed data distribution provides an unbiased foundation for estimation. This framework categorizes missingness into three classes: Missing Completely At Random (`MCAR`), Missing At Random (`MAR`), and Missing Not At Random (`MNAR`) (Van Buuren, 2012; Sportisse et al., 2020a;b). `MCAR` defines scenarios where missingness occurs uniformly and independently of all data values. `MAR` encompasses cases where missingness depends on observed variables that can be appropriately conditioned upon during analysis. `MNAR` describes situations where missingness depends on unobserved factors that cannot be easily conditioned on.

While this framework characterizes how missingness relates to the underlying data-generating process, it largely treats the missingness indicators for each variable as conditionally independent across entries. Recent work on structured missingness argues that, especially in large-scale multi-source

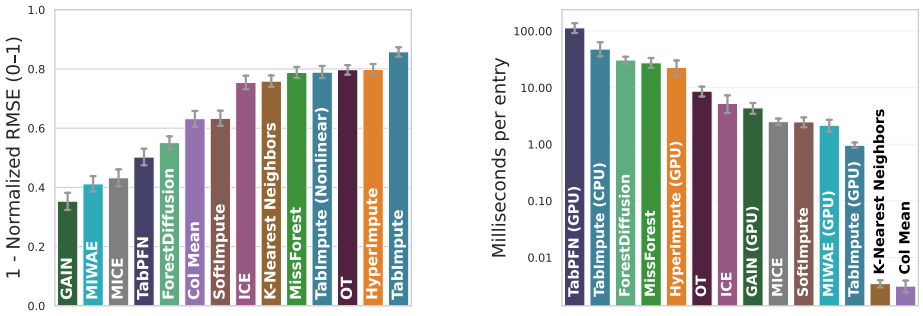

(a) Imputation Accuracy (↑) (b) Runtime (↓)

Figure 1: **Evaluation on real-world OpenML data: MissBench.** We compare TabImpute with 12 other popular methods on MissBench. In panel (a), we plot the imputation accuracy (defined as 1 - normalized RMSE), which is calculated for each method, normalized within a dataset, and averaged across datasets and 13 missingness patterns. Error bars indicate 95% confidence intervals. In panel (b), we compare the runtime per table entry. Any method not labeled (GPU) is tested on a CPU because that method is not implemented for GPUs. See Sec. 3 for our exact computing specifications and Sec. 4 for accuracy score methodology.

datasets, missingness itself can exhibit rich multivariate structure that is not captured by the standard MCAR/MAR/MNAR taxonomy. In particular, Mitra et al. (2023) introduce structured missingness as an umbrella term for mechanisms in which missingness follows systematic patterns. Jackson et al. (2023) provide a complementary characterization that allows dependencies among missingness indicators for different variables.

Previous work typically introduced new missingness patterns within these categories and proposed pattern-specific solutions. For instance, Agarwal et al. (2023) proposed a nearest neighbor-based matrix completion method specifically designed for a block-wise MNAR pattern. We instead develop a single method that performs well across diverse patterns and data domains by building on TabPFN, a popular tabular foundation model for supervised learning.

TabPFN is a pre-trained transformer model for supervised learning that performs well across a variety of domains without any fine-tuning (Hollmann et al., 2025). The team behind TabPFN created an imputation method in their `tabpfn-extensions` Python package by using the TabPFN model in iterative column-wise imputation (available on GitHub[1]). However, when evaluated on our new benchmark MissBench–consisting of 42 real-world OpenML datasets and 13 missingness patterns–TabPFN's imputation approach shows low accuracy and slow runtime. We improve on this approach by introducing a new entry-wise featurization (EWF), allowing parallel prediction of each missing value using TabPFN's model, denoted EWF-TabPFN. To further improve on EWF-TabPFN, we train a new underlying model specifically designed for tabular data imputation, TabImpute, to better fit this class of tasks, achieving the imputation accuracy shown in Fig. 1 and Tab. 1.

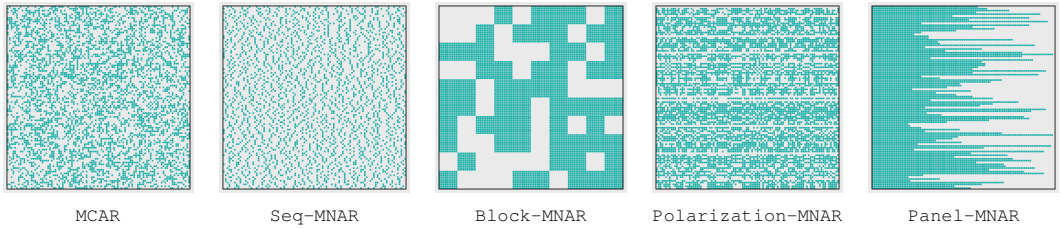

Figure 2: **Selection of synthetic missingness patterns implemented in MissBench.** Blue entries indicate observed values, and gray entries are unobserved.

[1] https://github.com/PriorLabs/tabpfn-extensions/blob/main/src/tabpfn_extensions/unsupervised/unsupervised.py

The main contributions of this work can be summarized as follows (also shown in Fig. 3):

- We propose a new state-of-the-art pre-trained transformer model, TabImpute, for missing data imputation by building on TabPFN and introducing a new entry-wise missing data featurization (see Sec. 3.1 for details).
- We develop a synthetic data generation pipeline to create training datasets with a comprehensive collection of missing values covering a wide range of MNAR patterns (see Sec. 3.2, App. A.2, and Tab. 9 for details).
- We demonstrate TabImpute's performance on a novel, comprehensive test bench, denoted MissBench, using 42 real-world OpenML datasets and 13 missingness patterns (see Sec. 4 for details). Our benchmark builds on previous work by testing more datasets and more missingness patterns: HyperImpute (Jarrett et al., 2022) tests on 13 UC Irvine (UCI) datasets (Kelly et al., 2024), a subset of OpenML, with 3 missingness patterns, and GAIN (Yoon et al., 2018) tests on 6 UCI datasets with 1 missingness pattern.

Our code and implementation details for all our contributions above can be accessed on GitHub.[2]

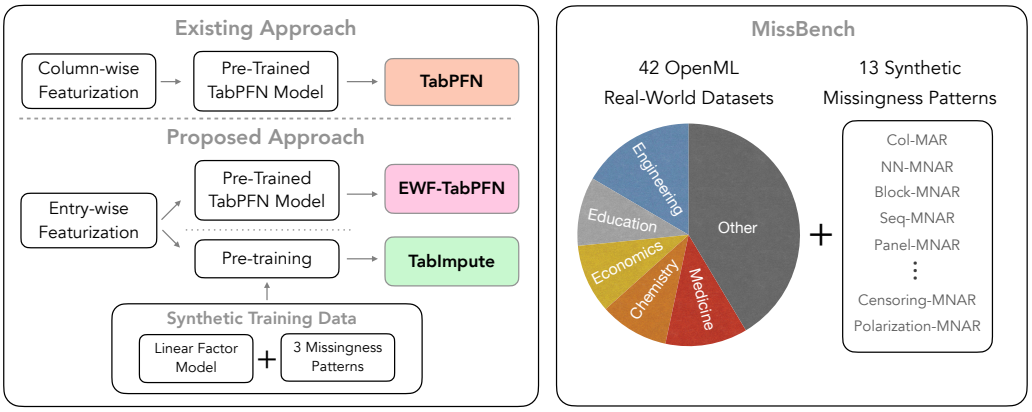

Figure 3: **Overview of our contributions.** The first row demonstrates TabPFN's imputation method, which performs iterative column-by-column imputation. We build on this by introducing an entry-wise featurization, as shown in the second row. We create a new synthetic data-generator for missingness data to train our model, TabImpute, shown in green (Sec. 3.2 and Sec. 3.3, respectively). We evaluate all the imputers on the comprehensive and rich set of OpenML datasets with many missingness patterns applied (Sec. 4).

1.1 Previous Work

We build primarily on missing data imputation and tabular representation learning (TRL). While missing data imputation is well-studied with established theory dating back to the 1970s (Rubin, 1976), TRL using tabular foundation models is relatively new (Müller et al., 2022; Zhang et al., 2025; Hollmann et al., 2023; 2025). Below, we describe relevant work that we directly compare against or build upon.

Imputation methods. Given the widespread nature of missing data, numerous imputation techniques have been proposed. These include averages, linear models over columns (Efron, 1994), random forest models (Hindy et al., 2024), ensemble methods (Jarrett et al., 2022), nearest neighbor-based methods (Chin et al., 2025), and even using generative adversarial networks (Yoon et al., 2018). For fully numerical data, matrix completion methods like SoftImpute (Hastie et al., 2015) have also been employed.

HyperImpute (Jarrett et al., 2022) combines the power of multiple classical imputation methods through iterative imputation (IM). IM loops over each column, using other columns to predict missing values until convergence. HyperImpute optimizes the imputer at each iteration over candidate

[2] https://anonymous.4open.science/r/tabular-6F65/README.md

methods, including MICE (Royston & White, 2011), SoftImpute (Hastie et al., 2015), column mean, MissForest (Stekhoven & Bühlmann, 2011), and Optimal Transport (Muzellec et al., 2020). While achieving great imputation accuracy across diverse missingness patterns and supporting categorical variables, HyperImpute is designed for supervised learning settings and cannot handle matrices with entirely missing columns (common in causal inference and panel data (Agarwal et al., 2023)). Additionally, optimization requires significantly more time than base methods.

Tabular representation learning. Tabular representation learning focuses on building models that can generalize across diverse tabular domains. The pioneering work in this area is TabPFN, a tabular foundation model for supervised learning. TabPFN was proposed in Hollmann et al. (2023) and subsequently improved in Hollmann et al. (2025). Since TabPFN's introduction, numerous variants have emerged to address scalability and performance limitations, as well as further work aimed at clarifying its internal representations (Zhang et al., 2025; Ye et al., 2025). Recent advances include TabICL (Qu et al., 2025), a scalable foundation model that extends supervised learning capabilities to datasets with up to 500K samples through a novel two-stage architecture with column-then-row attention mechanisms. Other notable models include MITRA (Zhang & Robinson, 2025), a tabular foundation model pre-trained on purely synthetic data from a mix of random classifiers/regressors, and Toto (Cohen et al., 2025), which is optimized for time series forecasting on observability metrics. Additionally, CausalFM (Ma et al., 2025) enables Bayesian causal inference through structural causal model priors similar to TabPFN, while DO-PFN (Robertson et al., 2025) extends the PFN framework to estimate counterfactual distributions from observational data.

2 Background on Prior-data Fitted Networks and TabPFN

Prior-data Fitted Networks (PFNs) are a class of models that learn to approximate Bayesian inference for a given prior (Müller et al., 2022). Instead of fitting a new model from scratch, a PFN is an individual, large pre-trained Transformer to perform classification or regression in a single forward pass. This process, known as in-context learning (ICL), allows the model to make predictions using sequences of labeled examples provided directly in the input, without requiring any gradient updates (Dong et al., 2024). The entire prediction algorithm is contained in the weights of the network, which is trained once on millions of synthetically generated datasets sampled from the prior. At inference time, the trained PFN takes a real-world dataset, composed of training and test samples, as a set-valued input and returns a distribution over the output space. This output space is categorical for classification tasks and the real line for regression tasks.

Posterior predictive modeling and synthetic prior fitting. PFNs are rooted in Bayesian supervised learning, where the primary objective is to model the posterior predictive distribution (PPD) (MacKay, 1992; Seeger, 2004; Blei et al., 2017). Since computing the PPD is often intractable (MacKay, 1992), PFNs instead learn to approximate the PPD offline through a process called synthetic prior fitting Müller et al. (2022). This is achieved using a prior specified by a sampling scheme that first samples a data-generating mechanism, $\phi \sim p(\phi)$, and then samples a synthetic dataset, $D \sim p(D|\phi)$. This process is repeated to generate millions of diverse datasets for training. The network's parameters, θ, are then optimized to predict held-out test samples ($D_{\text{test}} \subset D$) conditioned on the rest of the dataset ($D_{\text{train}} = D \setminus D_{\text{test}}$). The training objective is to minimize the negative log likelihood (NLL) loss on these held-out examples:

$$\mathcal{L}_{\text{NLL}}(\theta) = \mathbb{E}_{((x_{\text{test}}, y_{\text{test}}) \cup D_{\text{train}}) \sim p(D)}[-\log q_\theta(y_{\text{test}}|x_{\text{test}}, D_{\text{train}})].$$

This training process makes it explicit that PFNs are trained to emulate Bayesian inference by averaging over tasks drawn from a prior distribution over data-generating functions. Minimizing this loss ensures that the trained neural network, q_θ, learns to approximate the true Bayesian PPD for the specified prior.

TabPFN. TabPFN is a PFN built specifically for tabular supervised learning (Hollmann et al., 2023). The model employs a novel two-way attention mechanism specifically designed for tabular data. Unlike standard transformers (Vaswani et al., 2023) that treat tabular data as sequential tokens, TabPFN assigns separate representations to each cell in the table. The architecture uses alternating attention patterns: each cell first attends to other features within its row (inter-feature attention), then attends to the same feature across all rows (inter-sample attention). This design ensures permutation

invariance for both samples and features while enabling efficient scaling to larger tables than those seen during training. TabPFN v2 (Hollmann et al., 2025) retains the core training paradigm of the original TabPFN while introducing several key enhancements that improve accuracy, runtime, and applicability. Going forward, when referring to TabPFN, we mean TabPFN v2 since it is the most up-to-date version.

3 TRAINING TABIMPUTE ON SYNTHETIC DATA

We develop a featurization for tabular missing data imputation that enables better utilization of TabPFN's architecture, create a synthetic data generation pipeline across diverse missingness patterns, and employ an adaptive training algorithm to balance performance across all patterns. Training used 8 H200 GPUs and an Intel Xeon Platinum 8592+ CPU over approximately 2 days, processing 1.9 million synthetic tables. Our model matches TabPFN's size and runs on CPU-only systems. Evaluation used 1 H200 GPU.

3.1 ENTRY-WISE FEATURIZATION AND ARCHITECTURE

We recast missing data imputation as supervised learning to leverage TabPFN's architecture and enable parallel GPU computation of missing entries. For each dataset (training point), let X^* be the complete matrix with m rows and n columns, Ω be the set of missing entry indices, and X be the matrix with induced missingness:

$$X_{ij} = \begin{cases} X^*_{ij} & \text{for} \quad (i,j) \in [m] \times [n] \setminus \Omega \\ \star & \text{otherwise.} \end{cases}$$

where $\star$ denotes a missing entry. Let $\Omega_{\text{obs}} = [m] \times [n] \setminus \Omega$. Our feature matrix construction adds $(i \oplus j \oplus X_{i,:} \oplus X_{:,j})$ for each entry $i, j \in [m] \times [n]$, where $X_{i,:}$ denotes the i-th row, $X_{:,j}$ the j-th column, and $\oplus$ concatenation. Each row's target is $y_{ij} = X^*_{ij}$. During pre-training, we train the model to predict target values for all $(i, j) \in \Omega$. This procedure creates a feature matrix of size $nm \times (n + m)$. This featurization captures all necessary information for each cell through its row and column context while enabling parallel computation of missing entries on GPUs. Although the input matrix size increases, parallelization gains outweigh this cost.

Architecture. We use TabPFN's base architecture with one modification: removing the attention mask to allow input rows to attend to query rows. Since our input/query row sizes vary randomly with missingness patterns (unlike TabPFN's controlled synthetic generation), we remove the mask to enable parallel batch training. TabPFN's mask prevents train points from seeing test feature distributions, which is important in general supervised learning. However, our *test* set is created using data already available to the observed points, thus alleviating any data-leakage concerns.

3.2 SYNTHETIC TRAINING DATA GENERATION

We generate around 1.9 million matrices with missing values to train our model through a two-step process: first, generating underlying data, then introducing missingness patterns on top.

3.2.1 DATA GENERATION WITH LINEAR FACTOR MODELS

We generate data using a simple linear factor model (LFMs) (Bai & Ng, 2002). LFMs are commonly used in matrix completion literature to prove error bounds for matrix completion algorithms (Koren et al., 2009; Candes & Recht, 2012). This family of models generates a data matrix $Y \in \mathbb{R}^{m \times n}$ by assuming the data lies on or near a low-dimensional subspace. The simplest case generates the data matrix Y as the inner product of two lower-rank latent factor matrices, $U \in \mathbb{R}^{m \times k}$ and $V \in \mathbb{R}^{n \times k}$, where $k \ll n, m$ is the rank:

$$Y = UV^T.$$

To generate diverse datasets, the latent vectors (rows of U and V) are sampled from a variety of distributions, including Gaussian, Laplace, Student's t, spike-and-slab (a mixture of a Dirac delta at zero and a Gaussian), and Dirichlet.

When training, we experimented with several classes of data-generating processes (DGP), including matrices from nonlinear factor models and structural causal models (SCM) similar to the ones used in TabPFN. We found that training on SCM's proved too computationally expensive, but were able to train a model on nonlinear factor models. We found that the model trained on linear factor models performed the best, as shown in Tab. 8 in App. A.3. We leave it as future work to explore other DGPs which might further enhance the underlying model.

3.2.2 MISSINGNESS PATTERNS FOR TRAINING AND EVALUATION

After generating a complete data matrix $X^* \in \mathbb{R}^{m \times n}$, we introduce missingness by applying a masking matrix $M \in \{0,1\}^{m \times n}$, where the entry value $M_{ij} = 1$ if and only if $(i,j) \in \Omega_{\text{obs}}$. To ensure TabImpute is robust and generalizable to the variety of ways data can be missing in real-world scenarios, we pre-train on a comprehensive stock of synthetic datasets with several missingness patterns. For convenience, we define $p_{ij} = \mathbb{P}(M_{ij} = 1)$, the propensity of each entry in X^*.

We include 13 different missingness patterns: 1 `MCAR`, 1 `MAR` pattern, and 11 `MNAR` patterns. For examples of these, see Fig. 2. `MNAR` patterns often stump standard imputation methods and yet are extremely common in the real world.

`MCAR`: `MCAR` missingness means the probability of an entry being missing, defined as its propensity, is constant across entries and independent from any other randomness. The missingness indicators M_{ij} are drawn i.i.d. from a Bernoulli distribution $M_{ij} \sim \text{Bern}(p)$ across all $(i,j) \in [m] \times [n]$ for some constant $p \in (0,1)$. This is the simplest form of missingness, but is unrealistic (Van Buuren, 2012).

`MAR`: For `MAR` missingness, the probability of an entry being missing depends only on the observed values X. In other words, the randomness in `MAR` can be explained by conditioning on observed factors. Additionally, every entry has a positive probability of being observed (i.e., $p_{ij} > 0$). We simulate `MAR` through column-wise `MAR`, denoted `Col-MAR`: we choose several columns as predictor columns and use those values to mask entries in other columns. This is similar to the `MAR` approach taken in Jarrett et al. (2022).

`MNAR` Patterns: For the most complex missingness class, `MNAR`, the probability of an entry being missing can depend on unobserved factors. Note that `MNAR` patterns are significantly more difficult to handle systematically, often requiring specialized methods for a specific kind of `MNAR` pattern (Van Buuren, 2012). Due to the flexibility of our entry-wise featurization, TabImpute can produce imputations for these highly complex scenarios, even when columns are completely missing, such as in panel-data missingness patterns. HyperImpute was tested on two `MNAR` patterns in the Appendix of Jarrett et al. (2022), one where values are further masked after an `MAR` pattern and another where values outside a certain range are masked. We build on this work by testing on 11 `MNAR` patterns (see App. A.2 and Tab. 9 for details). We implement a range of `MNAR` patterns to simulate plausible real-world scenarios. For example, we utilize the expressiveness of neural networks to create random propensity functions `MNAR` patterns, use bandit algorithms to induce column-adaptive missing patterns, simulate panel data missingness where some features are removed later, censoring where sensor readings fall outside a detectable range, and survey data artifacts like respondent polarization and skip-logic.

3.3 TRAINING TABIMPUTE

We train our model to predict unobserved values under several missingness patterns simultaneously. For the final TabImpute model, we trained only on `MCAR` missingness because we found our model generalized to the other patterns well without including them explicitly in training. In fact, we found that including other missingness patterns degraded overall performance. We discuss these results further below. We use the prior-data fitted negative log likelihood (NLL) loss proposed in Müller et al. (2022). Like other PFNs with continuous numerical output, we use the Riemann distribution output also proposed in Müller et al. (2022). Since we can generate an unlimited amount of synthetic data, we do not reuse any synthetic data and only do one gradient pass per batch of datasets. This allows our model to learn the underlying data-generating process and missingness

mechanisms without risk of memorization. We use a learning rate of 0.0001, a batch size of 16, and train on around 1.9 million synthetic datasets.

Remark: We had initially attempted to train the model sequentially on one missingness pattern at a time, but found that the network always experienced *catastrophic forgetting* (McCloskey & Cohen, 1989) irrespective of learning rate (i.e., it forgot how to handle the previous missingness patterns). After this, we attempted to mix several missingness types together: `MCAR`, `MAR`, and `Self-Masking-MNAR`. However, we found that the model's performance degraded overall because it focused only `Self-Masking-MNAR`. We attempted several mitigation techniques including pattern weight schedules and GradNorm Chen et al. (2018), a gradient normalization technique for multi-task learning, but found them unsuccessful in improving performance.

4 Results on OpenML Datasets: MissBench

To evaluate TabImpute against other methods, we introduce MissBench: a missing-data imputation benchmark using 42 OpenML (Vanschoren et al., 2013) tabular datasets with 13 synthetic missingness patterns. For every dataset and missingness pattern, we test each method's ability to impute masked values. The 42 OpenML datasets span domains such as medicine, engineering, and education. The missingness patterns include 1 `MCAR` pattern, 1 `MAR` pattern, and 11 `MNAR` patterns. We provide details for the `MNAR` patterns in App. A.2.

We test a suite of imputation methods on MissBench: column-mean imputation (Hawthorne & Elliott, 2005), SoftImpute (Hastie et al., 2015), MissForest (Stekhoven & Bühlmann, 2011), iterative chained estimators (ICE/MICE) (van Buuren & Groothuis-Oudshoorn, 2011; Royston & White, 2011), GAIN (Yoon et al., 2018), MIWAE (Mattei & Frellsen, 2019), an optimal transport-based method (Muzellec et al., 2020), and TabPFN's imputation method (see Sec. 1). We also test imputing categorical variables via one-hot encoding in App. A.1 and report R^2 values in Tab. 7.

Imputation Accuracy. To ensure a fair comparison across datasets with different scales and inherent difficulties, we report a normalized accuracy score. In particular, for each dataset and missingness pattern, we first calculate the standard Root Mean Squared Error (RMSE) for every imputation method as $\left(\frac{1}{|\Omega|}\sum_{(i,j)\in\Omega}\left(X_{ij}^{\text{true}} - X_{ij}^{\text{imputed}}\right)^2\right)^{1/2}$, where Ω denotes the set of missing entries. We then perform a min-max normalization on these RMSE scores across all methods for that specific task:

$$\text{Normalized RMSE} = \frac{\text{RMSE}_{\text{method}} - \min(\text{RMSE}_{\text{all methods}})}{\max(\text{RMSE}_{\text{all methods}}) - \min(\text{RMSE}_{\text{all methods}})}$$

This normalization maps the best-performing method to 0 and the worst to 1. Finally, we define *Imputation Accuracy* as $1 -$ Normalized RMSE, where higher values indicate better performance.

The final scores we report represent imputation accuracy averaged across all 42 datasets and 13 missingness patterns. Dataset sizes range from 50×5 to 170×55. We evaluate only on datasets with numerical values without pre-existing missingness before applying synthetic patterns. Specific datasets are listed in Tab. 10 (App. A.3).

Tab. 1 presents results for each missingness pattern as well as overall performance. TabImpute achieves the best overall performance and for nearly all individual patterns. For completeness, we list the performance of methods not shown in the table in Tab. 6 and non-normalized RMSE values in Tab. 11. TabImpute performs best under high missingness conditions (Fig. 4, App. A.1), which is expected since it leverages generative pre-training rather than relying solely on available dataset information like discriminative methods.

Multiple imputation (MI) Metrics. In multiple imputation, a dataset is imputed multiple times independently. These datasets can then be used to provide better confidence intervals of downstream quantities Van Buuren (2012). Given two imputation methods that have the same imputation accuracy, one would prefer a method with higher uncertainty to not provide false precision on imputed values Van Buuren (2012); Li et al. (2015); Jolicoeur-Martineau et al. (2024). We assess performance for multiple imputation by repeating imputation 5 times per dataset and calculating the median absolute deviation (MAD), minimimum RMSE, and average RMSE, shown in Tab. 2. While

Table 1: Imputation Accuracy ± Standard Error by Missingness Pattern.
We train on the pattern above the dashed line. The number of samples used to calculate standard error are the number of datasets: 42.

Pattern	TabImpute	EWF-TabPFN	HyperImpute	MissForest
MCAR	**0.882 ± 0.021**	0.817 ± 0.024	0.804 ± 0.031	0.867 ± 0.022
NN-MNAR	**0.900 ± 0.019**	0.876 ± 0.020	0.760 ± 0.036	0.818 ± 0.029
Self-Masking-MNAR	**0.703 ± 0.038**	0.682 ± 0.042	0.689 ± 0.039	0.638 ± 0.040
Col-MAR	**0.877 ± 0.030**	0.855 ± 0.027	0.814 ± 0.040	0.773 ± 0.039
Block-MNAR	0.890 ± 0.026	**0.905 ± 0.026**	0.873 ± 0.027	0.860 ± 0.023
Seq-MNAR	**0.920 ± 0.014**	0.905 ± 0.015	0.864 ± 0.030	0.829 ± 0.031
Panel-MNAR	**0.915 ± 0.025**	0.711 ± 0.048	0.865 ± 0.033	0.912 ± 0.020
Polarization-MNAR	0.804 ± 0.024	**0.879 ± 0.021**	0.622 ± 0.039	0.567 ± 0.033
Soft-Polarization-MNAR	0.759 ± 0.045	**0.864 ± 0.024**	0.711 ± 0.034	0.667 ± 0.041
Latent-Factor-MNAR	**0.891 ± 0.021**	0.883 ± 0.018	0.775 ± 0.036	0.834 ± 0.023
Cluster-MNAR	**0.903 ± 0.014**	0.871 ± 0.021	0.839 ± 0.028	0.830 ± 0.021
Two-Phase-MNAR	**0.886 ± 0.026**	0.851 ± 0.029	0.865 ± 0.031	0.873 ± 0.020
Censoring-MNAR	0.710 ± 0.032	0.593 ± 0.045	**0.786 ± 0.041**	0.671 ± 0.038
Overall	**0.849 ± 0.008**	0.823 ± 0.009	0.790 ± 0.010	0.780 ± 0.009

most imputation methods require another full run in order to create another imputation, TabImpute and other PFN-based methods output a distribution. This distribution is then sampled 5 times to create 5 different imputations, following the methodology of ForestDiffusion Jolicoeur-Martineau et al. (2024). Thus, multiple imputation for TabImpute uses the same runtime as a single imputation.

TabImpute provides better diversity than methods of comparable imputation accuracy (MissForest and HyperImpute). The poor precision of MissForest and HyperImpute is shown through their worse minimum RMSE values. Note that in Tab. 2, TabImpute has a higher avergage RMSE value then MissForest and HyperImpute. This is because it has a higher diversity in its estimate (the samples have a larger spread). When comparing just the median estimate, though, TabImpute has a better accuracy, as shown in the first row in Tab. 1. Thus, TabImpute provides practitioners with the best of both worlds: If they require multiple imputation for uncertainty estimates, TabImpute provides diverse estimates, and if they require a single good imputation, TabImpute provides the most accurate estimate.

Table 2: Multiple Imputation Metrics: Dataset-level MAD and RMSE Metrics ± Standard Error per Imputed Entry Across 5 Samples (MCAR, p=0.4).

Method	MAD (↑)	Min RMSE (↓)	Avg RMSE (↓)
MICE	**0.359 ± 0.002**	**0.264 ± 0.003**	0.859 ± 0.005
MIWAE	0.267 ± 0.001	0.385 ± 0.005	0.927 ± 0.005
GAIN	0.200 ± 0.001	0.361 ± 0.004	0.789 ± 0.005
TabImpute	0.199 ± 0.002	0.337 ± 0.004	0.722 ± 0.006
ForestDiffusion	0.181 ± 0.001	0.291 ± 0.004	0.739 ± 0.005
OT	0.049 ± 0.000	0.440 ± 0.005	0.547 ± 0.005
HyperImpute	0.037 ± 0.001	0.420 ± 0.004	0.551 ± 0.005
MissForest	0.036 ± 0.000	0.434 ± 0.005	**0.532 ± 0.005**
SoftImpute	0.001 ± 0.000	0.577 ± 0.005	0.649 ± 0.005
Col Mean	0.000 ± 0.000	0.813 ± 0.005	0.813 ± 0.005
ICE	0.000 ± 0.000	0.606 ± 0.005	0.606 ± 0.005

Specialized TabImpute Models. After training TabImpute on the MCAR pattern, we attempted to improve it by mixing in Col-MAR and Self-Masking-MNAR in the pre-training process. However, we found that the model consistently collapsed to only learning Self-Masking-MNAR, degrading performance on other patterns. This new model, though, performed far better on Self-Masking-MNAR than any other method, demonstrating the power of this architecture and

pre-training to learn any pattern. We show the relative performance of three models trained on MCAR, Col-MAR, and Self-Masking-MNAR, respectively, in Tab. 3.

The model trained on Self-Masking-MNAR performs much better than the other models on this pattern. However, it does not generalize well to other patterns because the masks generated by the Self-Masking-MNAR pattern do not cover the types of masks generated by other patterns. On the other hand, when generating MCAR patterns millions of times, a small portion of these masks will look like Self-Masking-MNAR masks. Interestingly, the MCAR-trained model performed slightly better on Col-MAR patterns than the model trained on Col-MAR exclusively. One explanation for this is that the masks generated under MAR pattern are covered well by MCAR masks and MCAR masks produce a better underlying model. Note that the imputation accuracy scores are different for Tab. 1 and Tab. 3 because the MAR and Self-Masking-MNAR models are not included in the normalization in Tab. 1. However, the order of the imputation accuracy remains consistent.

Remark: We implemented an ensembling approach which weighted specialized model outputs by how well they predicted the observed values within a matrix, but found this approach to always favor the MCAR-trained model. We leave it for future work to determine a better method for ensembling or routing the specialized model predictions to better take advantage of specialized models.

Table 3: Imputation Accuracy ± Standard Error by Missingness Pattern for Specialized Models

Pattern	$\text{TabImpute}_{\texttt{MCAR}}$	$\text{TabImpute}_{\texttt{Col-MAR}}$	$\text{TabImpute}_{\texttt{Self-Masking-MNAR}}$
MCAR	**0.938 ± 0.028**	0.832 ± 0.024	0.020 ± 0.020
Self-Masking-MNAR	0.463 ± 0.067	0.329 ± 0.065	**0.624 ± 0.072**
Col-MAR	**0.899 ± 0.042**	0.811 ± 0.050	0.081 ± 0.041
Overall	**0.766 ± 0.034**	0.656 ± 0.035	0.243 ± 0.037

5 Conclusion & Future Work

In this paper, we present a state-of-the-art pre-trained transformer for the tabular missing data problem. We build on recent work in tabular representation learning by adapting TabPFN's architecture and training pipeline for the missing data setting. Even though we train purely on synthetic data, we are able to impute entries accurately on real-world OpenML data for a comprehensive set of missingness patterns, thus showcasing our model's ability to generalize to unseen domains. We open-source not only our model architecture and weights, but also our training and evaluation code (available at https://anonymous.4open.science/r/tabular-6F65/README.md). We hope this will facilitate others to validate, utilize, and build upon our work.

Since we use the same architecture as TabPFN, we also suffer from the quadratic time complexity of attention along both rows and columns. Due to entry-wise featurization, this complexity is squared again along the row axis. While TabImpute proved to be fast on relatively small tables in MissBench, we expect scalability to be a concern on larger table sizes. Additionally, TabImpute is very fast when using a GPU, but is slower on a CPU similar to TabPFN. This can be partly alleviated by imputing tables in chunks, but we leave this for future work.

Note that since we utilize a base architecture similar to TabPFN, any further improvements to TabPFN's architecture can be immediately ported to TabImpute. For example, Zeng et al. (2025) and Qu et al. (2025) propose different attention mechanisms to speed up TabPFN-like architectures for tabular data. Finally, since we use a PFN architecture, we output a distribution for each missing entry and can sample from this distribution for multiple imputation (Rubin, 2018). In future work, we plan on (i) exploring training further on more complex missingness patterns and data-generating processes, (ii) enhancing our method to impute categorical data better, (iii) extending our evaluation set to causal inference settings, which can be modeled as missing-data problems (Agarwal et al., 2023), (iv) improving the architecture to scale to larger datasets, and (v) utilizing TabImpute further for multiple imputation datasets.

Reproducibility Statement. We open-source our training code, evaluation code, model architecture and weights, and synthetic data-generation pipeline (available at `https://anonymous.4open.science/r/tabular-6F65/`). While we utilize 8 H200 GPUs to train our model, our model should be able to fit easily on GPUs with far less memory because our model only has around 22 million parameters. All of the datasets we use for evaluation are public and available in OpenML, making it straightforward to reproduce our results from our pre-trained model.

REFERENCES

Anish Agarwal, Munther Dahleh, Devavrat Shah, and Dennis Shen. Causal matrix completion. In *The thirty sixth annual conference on learning theory*, pp. 3821–3826. PMLR, 2023.

Peter Auer, Nicolo Cesa-Bianchi, and Paul Fischer. Finite-time analysis of the multiarmed bandit problem. *Machine learning*, 47(2):235–256, 2002.

Jushan Bai and Serena Ng. Determining the number of factors in approximate factor models. *Econometrica*, 70(1):191–221, 2002. doi: https://doi.org/10.1111/1468-0262.00273. URL https://onlinelibrary.wiley.com/doi/abs/10.1111/1468-0262.00273.

Gustavo E. A. P. A. Batista and Maria Carolina Monard. An analysis of four missing data treatment methods for supervised learning. *Applied Artificial Intelligence*, 17(5-6):519–533, 2003. doi: 10.1080/713827181. URL https://doi.org/10.1080/713827181.

Jelke Bethlehem. Selection bias in web surveys. *International statistical review*, 78(2):161–188, 2010.

David M Blei, Alp Kucukelbir, and Jon D McAuliffe. Variational inference: A review for statisticians. *Journal of the American statistical Association*, 112(518):859–877, 2017.

Emmanuel Candes and Benjamin Recht. Exact matrix completion via convex optimization. *Communications of the ACM*, 55(6):111–119, 2012.

Amnon Cavari and Guy Freedman. Survey nonresponse and mass polarization: The consequences of declining contact and cooperation rates. *American Political Science Review*, 117(1):332–339, 2023.

Haiying Chen, Sara A Quandt, Joseph G Grzywacz, and Thomas A Arcury. A bayesian multiple imputation method for handling longitudinal pesticide data with values below the limit of detection. *Environmetrics*, 24(2):132–142, 2013.

Zhao Chen, Vijay Badrinarayanan, Chen-Yu Lee, and Andrew Rabinovich. Gradnorm: Gradient normalization for adaptive loss balancing in deep multitask networks. In *International conference on machine learning*, pp. 794–803. PMLR, 2018.

Caleb Chin, Aashish Khubchandani, Harshvardhan Maskara, Kyuseong Choi, Jacob Feitelberg, Albert Gong, Manit Paul, Tathagata Sadhukhan, Anish Agarwal, and Raaz Dwivedi. N^2: A unified python package and test bench for nearest neighbor-based matrix completion. *arXiv preprint arXiv:2506.04166*, 2025.

Ben Cohen, Emaad Khwaja, Youssef Doubli, Salahidine Lemaachi, Chris Lettieri, Charles Masson, Hugo Miccinilli, Elise Ramé, Qiqi Ren, Afshin Rostamizadeh, Jean Ogier du Terrail, Anna-Monica Toon, Kan Wang, Stephan Xie, Zongzhe Xu, Viktoriya Zhukova, David Asker, Ameet Talwalkar, and Othmane Abou-Amal. This time is different: An observability perspective on time series foundation models, 2025. URL https://arxiv.org/abs/2505.14766.

Karla Diaz-Ordaz, Michael G Kenward, Abie Cohen, Claire L Coleman, and Sandra Eldridge. Are missing data adequately handled in cluster randomised trials? a systematic review and guidelines. *Clinical Trials*, 11(5):590–600, 2014.

Qingxiu Dong, Lei Li, Damai Dai, Ce Zheng, Jingyuan Ma, Rui Li, Heming Xia, Jingjing Xu, Zhiyong Wu, Tianyu Liu, Baobao Chang, Xu Sun, Lei Li, and Zhifang Sui. A survey on in-context learning, 2024. URL https://arxiv.org/abs/2301.00234.

Bradley Efron. Missing data, imputation, and the bootstrap. *Journal of the American Statistical Association*, 89(426):463–475, 1994.

Craig K Enders, Stephen A Mistler, and Brian T Keller. Multilevel multiple imputation: A review and evaluation of joint modeling and chained equations imputation. *Psychological methods*, 21 (2):222, 2016.

Evelyn Fix and J. L. Hodges. Discriminatory analysis. nonparametric discrimination: Consistency properties. *International Statistical Review / Revue Internationale de Statistique*, 57(3):238–247, 1989. ISSN 03067734, 17515823. URL http://www.jstor.org/stable/1403797.

Susobhan Ghosh, Raphael Kim, Prasidh Chhabria, Raaz Dwivedi, Predrag Klasnja, Peng Liao, Kelly Zhang, and Susan Murphy. Did we personalize? assessing personalization by an online reinforcement learning algorithm using resampling. *Machine learning*, 113(7):3961–3997, 2024.

Ian Goodfellow, Jean Pouget-Abadie, Mehdi Mirza, Bing Xu, David Warde-Farley, Sherjil Ozair, Aaron Courville, and Yoshua Bengio. Generative adversarial networks. *Communications of the ACM*, 63(11):139–144, 2020.

John W Graham, Bonnie J Taylor, Allison E Olchowski, and Patricio E Cumsille. Planned missing data designs in psychological research. *Psychological methods*, 11(4):323, 2006.

Trevor Hastie, Rahul Mazumder, Jason D Lee, and Reza Zadeh. Matrix completion and low-rank svd via fast alternating least squares. *The Journal of Machine Learning Research*, 16(1):3367–3402, 2015.

Jerry A Hausman and David A Wise. Attrition bias in experimental and panel data: the gary income maintenance experiment. *Econometrica: Journal of the Econometric Society*, pp. 455–473, 1979.

Graeme Hawthorne and Peter Elliott. Imputing cross-sectional missing data: comparison of common techniques. *Australian & New Zealand Journal of Psychiatry*, 39(7):583–590, 2005.

Dennis R Helsel. *Statistics for censored environmental data using Minitab and R*, volume 77. John Wiley & Sons, 2011.

Hindy, Mario Villaizan Vallelado, and Sep905. yuenshingyan/missforest: Missforest in python - arguably the best missing values imputation method, August 2024. URL https://doi.org/10.5281/zenodo.13368883.

Noah Hollmann, Samuel Müller, Katharina Eggensperger, and Frank Hutter. TabPFN: A transformer that solves small tabular classification problems in a second. In *The Eleventh International Conference on Learning Representations*, 2023. URL https://openreview.net/forum?id=cp5PvcI6w8_.

Noah Hollmann, Samuel Müller, Lennart Purucker, Arjun Krishnakumar, Max Körfer, Shi Bin Hoo, Robin Tibor Schirrmeister, and Frank Hutter. Accurate predictions on small data with a tabular foundation model. *Nature*, 637(8045):319–326, 2025.

Nan Hu, Jie Zhang, and Paul A Pavlou. Overcoming the j-shaped distribution of product reviews. *Communications of the ACM*, 52(10):144–147, 2009.

Joseph G Ibrahim and Geert Molenberghs. Missing data methods in longitudinal studies: a review. *Test*, 18(1):1–43, 2009.

Joseph G Ibrahim, Ming-Hui Chen, Stuart R Lipsitz, and Amy H Herring. Missing-data methods for generalized linear models. *Journal of the American Statistical Association*, 100(469): 332–346, 2005. doi: 10.1198/016214504000001844. URL https://doi.org/10.1198/016214504000001844.

James Jackson, Robin Mitra, Niels Hagenbuch, Sarah McGough, and Chris Harbron. A complete characterisation of structured missingness, 2023. URL https://arxiv.org/abs/2307.02650.

Daniel Jarrett, Bogdan C Cebere, Tennison Liu, Alicia Curth, and Mihaela van der Schaar. Hyperimpute: Generalized iterative imputation with automatic model selection. In *International Conference on Machine Learning*, pp. 9916–9937. PMLR, 2022.

Huaqing Jin, Yanyuan Ma, and Fei Jiang. Matrix completion with covariate information and informative missingness. *Journal of Machine Learning Research*, 23(180):1–62, 2022.

Alexia Jolicoeur-Martineau, Kilian Fatras, and Tal Kachman. Generating and imputing tabular data via diffusion and flow-based gradient-boosted trees. In *International conference on artificial intelligence and statistics*, pp. 1288–1296. PMLR, 2024.

Yuliya Karpievitch, Jeff Stanley, Thomas Taverner, Jianhua Huang, Joshua N Adkins, Charles Ansong, Fred Heffron, Thomas O Metz, Wei-Jun Qian, Hyunjin Yoon, et al. A statistical framework for protein quantitation in bottom-up ms-based proteomics. *Bioinformatics*, 25(16):2028–2034, 2009.

Markelle Kelly, Rachel Longjohn, and Kolby Nottingham. The uci machine learning repository. `https://archive.ics.uci.edu`, 2024. Accessed: 2025-09-19.

Yehuda Koren, Robert Bell, and Chris Volinsky. Matrix factorization techniques for recommender systems. *Computer*, 42(8):30–37, 2009. doi: 10.1109/MC.2009.263.

Tor Lattimore and Csaba Szepesvári. *Bandit algorithms*. Cambridge University Press, 2020.

Cosmin Lazar, Laurent Gatto, Myriam Ferro, Christophe Bruley, and Thomas Burger. Accounting for the multiple natures of missing values in label-free quantitative proteomics data sets to compare imputation strategies. *Journal of proteome research*, 15(4):1116–1125, 2016.

Peng Li, Elizabeth A Stuart, and David B Allison. Multiple imputation: a flexible tool for handling missing data. *Jama*, 314(18):1966–1967, 2015.

Roderick JA Little. Modeling the drop-out mechanism in repeated-measures studies. *Journal of the american statistical association*, 90(431):1112–1121, 1995.

Roderick JA Little and Donald B Rubin. *Statistical analysis with missing data*. John Wiley & Sons, 2019.

Yuchen Ma, Dennis Frauen, Emil Javurek, and Stefan Feuerriegel. Foundation models for causal inference via prior-data fitted networks, 2025. URL `https://arxiv.org/abs/2506.10914`.

David JC MacKay. A practical bayesian framework for backpropagation networks. *Neural computation*, 4(3):448–472, 1992.

Benjamin M Marlin and Richard S Zemel. Collaborative prediction and ranking with non-random missing data. In *Proceedings of the third ACM conference on Recommender systems*, pp. 5–12, 2009.

Pierre-Alexandre Mattei and Jes Frellsen. Miwae: Deep generative modelling and imputation of incomplete data sets. In *International Conference on Machine Learning*, pp. 4413–4423. PMLR, 2019.

Michael McCloskey and Neal J Cohen. Catastrophic interference in connectionist networks: The sequential learning problem. In *Psychology of learning and motivation*, volume 24, pp. 109–165. Elsevier, 1989.

Robin Mitra, Sarah F McGough, Tapabrata Chakraborti, Chris Holmes, Ryan Copping, Niels Hagenbuch, Stefanie Biedermann, Jack Noonan, Brieuc Lehmann, Aditi Shenvi, et al. Learning from data with structured missingness. *Nature Machine Intelligence*, 5(1):13–23, 2023.

K. Mohan. On handling self-masking and other hard missing data problems. In *AAAI Symposium 2018*, 2018.

Jeffrey C Moore and Edward J Welniak. Income measurement error in surveys: A review. *Journal of official statistics*, 16(4):331, 2000.

Samuel Müller, Noah Hollmann, Sebastian Pineda Arango, Josif Grabocka, and Frank Hutter. Transformers can do bayesian inference. In *International Conference on Learning Representations*, 2022. URL `https://openreview.net/forum?id=KSugKcbNf9`.

Boris Muzellec, Julie Josse, Claire Boyer, and Marco Cuturi. Missing data imputation using optimal transport. In *International Conference on Machine Learning*, pp. 7130–7140. PMLR, 2020.

Jerzy Neyman. Contribution to the theory of sampling human populations. *Journal of the American Statistical Association*, 33(201):101–116, 1938.

Jingang Qu, David Holzmüller, Gaël Varoquaux, and Marine Le Morvan. Tabicl: A tabular foundation model for in-context learning on large data. *arXiv preprint arXiv:2502.05564*, 2025.

Mijke Rhemtulla and Gregory R Hancock. Planned missing data designs in educational psychology research. *Educational Psychologist*, 51(3-4):305–316, 2016.

Jake Robertson, Arik Reuter, Siyuan Guo, Noah Hollmann, Frank Hutter, and Bernhard Schölkopf. Do-pfn: In-context learning for causal effect estimation, 2025. URL https://arxiv.org/abs/2506.06039.

Patrick Royston and Ian R White. Multiple imputation by chained equations (mice): implementation in stata. *Journal of statistical software*, 45:1–20, 2011.

Donald B Rubin. Inference and missing data. *Biometrika*, 63(3):581–592, 1976.

Donald B Rubin. Multiple imputation. In *Flexible imputation of missing data, second edition*, pp. 29–62. Chapman and Hall/CRC, 2018.

Tobias Schnabel, Adith Swaminathan, Ashudeep Singh, Navin Chandak, and Thorsten Joachims. Recommendations as treatments: Debiasing learning and evaluation. In *international conference on machine learning*, pp. 1670–1679. PMLR, 2016.

Matthias Seeger. Gaussian processes for machine learning. *International journal of neural systems*, 14(02):69–106, 2004.

Aude Sportisse, Claire Boyer, and Julie Josse. Imputation and low-rank estimation with missing not at random data. *Statistics and Computing*, 30(6):1629–1643, 2020a.

Aude Sportisse, Claire Boyer, and Julie Josse. Estimation and imputation in probabilistic principal component analysis with missing not at random data. In H. Larochelle, M. Ranzato, R. Hadsell, M.F. Balcan, and H. Lin (eds.), *Advances in Neural Information Processing Systems*, volume 33, pp. 7067–7077. Curran Associates, Inc., 2020b. URL https://proceedings.neurips.cc/paper_files/paper/2020/file/4ecb679fd35dcfd0f0894c399590be1a-Paper.pdf.

Harald Steck. Training and testing of recommender systems on data missing not at random. In *Proceedings of the 16th ACM SIGKDD international conference on Knowledge discovery and data mining*, pp. 713–722, 2010.

Daniel J. Stekhoven and Peter Bühlmann. Missforest—non-parametric missing value imputation for mixed-type data. *Bioinformatics*, 28(1):112–118, 10 2011.

William R Thompson. On the likelihood that one unknown probability exceeds another in view of the evidence of two samples. *Biometrika*, 25(3/4):285–294, 1933.

Stef Van Buuren. Multiple imputation of multilevel data. In *Handbook of advanced multilevel analysis*, pp. 173–196. Routledge, 2011.

Stef Van Buuren. *Flexible imputation of missing data*, volume 10. CRC press Boca Raton, FL, 2012.

Stef van Buuren and Karin Groothuis-Oudshoorn. Mice: Multivariate imputation by chained equations in r. *Journal of Statistical Software*, 45(3):1–67, 2011. doi: 10.18637/jss.v045.i03. URL https://www.jstatsoft.org/index.php/jss/article/view/v045i03.

Joaquin Vanschoren, Jan N. van Rijn, Bernd Bischl, and Luis Torgo. Openml: Networked science in machine learning. *SIGKDD Explorations*, 15(2):49–60, 2013. doi: 10.1145/2641190.2641198. URL http://doi.acm.org/10.1145/2641190.2641198.

Ashish Vaswani, Noam Shazeer, Niki Parmar, Jakob Uszkoreit, Llion Jones, Aidan N. Gomez, Lukasz Kaiser, and Illia Polosukhin. Attention is all you need, 2023. URL https://arxiv.org/abs/1706.03762.

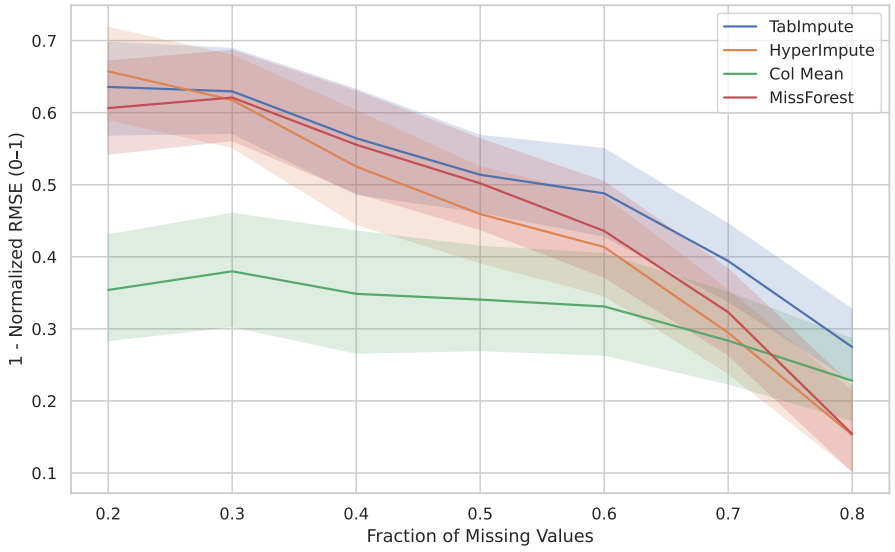

Figure 4: **Imputation Accuracy vs. probability of missingness for `MCAR`.** TabImpute performs the best when missingness is higher because it is a generative model that fits to the data in-context.

Han-Jia Ye, Si-Yang Liu, and Wei-Lun Chao. A closer look at tabpfn v2: Strength, limitation, and extension. *arXiv preprint arXiv:2502.17361*, 2025.

Jinsung Yoon, James Jordon, and Mihaela van der Schaar. Gain: Missing data imputation using generative adversarial nets. In *International Conference on Machine Learning (ICML)*, 2018.

Yuchen Zeng, Tuan Dinh, Wonjun Kang, and Andreas C Mueller. Tabflex: Scaling tabular learning to millions with linear attention. *arXiv preprint arXiv:2506.05584*, 2025.

Qiong Zhang, Yan Shuo Tan, Qinglong Tian, and Pengfei Li. Tabpfn: One model to rule them all?, 2025. URL `https://arxiv.org/abs/2505.20003`.

Xiyuan Zhang and Danielle Maddix Robinson. Mitra: Mixed synthetic priors for enhancing tabular foundation models, Jul 2025. URL `https://www.amazon.science/blog/mitra-mixed-synthetic-priors-for-enhancing-tabular-foundation-models`.

A Appendix

Here we present the rest of the missingness patterns we tested on, tables with further results, the methods we tested against, and the OpenML datasets we evaluated on.

A.1 Additional tests

Next, we discuss when TabImpute does well and when HyperImpute and other methods do well. We found that an important factor in determining performance was the level of missingness. The probability of missingness can only be controlled precisely for `MCAR`. Thus, we show in Fig. 4 the performance of the top methods as we increase the missingness level.

Support for categorical variables. We support imputing categorical variables via one-hot encodings: First, we convert each categorical column into several one-hot encoding columns. Then, we impute missing entries within this now purely numerical matrix. We then choose the class with the highest score as the categorical imputation for that missing entry. Note that we could also perform

a softmax operation over the imputed scores within the one-hot encoded columns to output probabilities over classes. With this method, TabImpute achieves AUC close to that of MissForest and HyperImpute when tested on MCAR missingness with $p = 0.4$, as shown in Tab. 4. We leave it for future work to incorporate categorical features into the training procedure, which would likely improve TabImpute's performance.

A.2 Details for MNAR Missingness Patterns

This section provides the mathematical and implementation details for each of the simulated MNAR missingness mechanisms that we implement and test. For each pattern, we define the mechanism by which the missingness mask M is generated, where $M_{ij} = 1$ if the value X_{ij} is observed and $M_{ij} = 0$ otherwise.

A.2.1 Details for NN-MNAR

Description This pattern simulates a scenario where the propensity p_{ij} depends on the underlying matrix values X^* in an arbitrary manner. We achieve a comprehensive coverage of MNAR patterns by leveraging the expressiveness of neural networks.

Methodology One general form of MNAR can be described as follows: for all i and j, there exists some function f_{ij} on the true (hence unobserved) matrix X^* such that the propensity depends on X^* as follows: $p_{ij}(X^*) = \mathbb{P}(M_{ij} = 1|X^*) = f_{ij}(X^*)$. By leveraging the expressiveness of neural networks, we propose a neural-net-based MAR pattern generator (NN-MNAR) that is designed to approximate arbitrary propensities characterized by functions f_{ij}.

Implementation Details For fixed indices i and j, NN-MNARconstructs the propensity p_{ij} in a two-step procedure. First, we randomly collect a subset of values from the matrix X^* and flatten them as a vector, say $X^*(i, j)$; we do this by first randomly generating a neighborhood $\mathbf{N}_{ij} \subset [m] \times [n]$, then the entries in the neighborhood $X^*_{st}, (s, t) \in \mathbf{N}_{ij}$ constitute the entries of the vector $X^*(i, j)$. Second, a neural-net function $g_{ij} : \mathbb{R}^{|\mathbf{N}_{ij}|} \to [0, 1]$ is constructed by randomly initializing the number of layers, depth, weight, and bias. At each training step, the random neighborhood $\mathbf{N}_{ij}$ and the random neural-net g_{ij} collectively defines the propensity $p_{ij} = g_{ij}(X^*(i, j))$ from which MNAR missingness patterns are generated $M_{ij} \sim \mathrm{Bern}(p_{ij})$.

A.2.2 Details on Seq-MNAR

Description This pattern simulates a scenario where masking matrix values $M_{ij} \in \{0, 1\}$ for each column j are adaptively chosen depending on the information up to column $j - 1$ (i.e., regard columns as time). Specifically, we employ variants of bandit algorithms Lattimore & Szepesvári (2020) while regarding the binary masking matrix values as the two arms. Such patterns commonly arise in sequential experiments Ghosh et al. (2024).

Methodology The true matrix X^* is transformed to constitute the reward. For each designated column j, one of the following bandit algorithm utilizes the all the information of X^* and M up to column $j - 1$ and chooses one of the two arms $\{0, 1\}$ via one of the following algorithms: ε-greedy, upper-confidence bound (UCB), Thompson-sampling (Thompson, 1933) or gradient bandit.

Implementation Details We generate exogenous Gaussian noise and add it to the true matrix X^* and regard X^* as the reward for arm 0 and its noisy version as the reward for arm 1. Then, starting from the first column with multiple rows as multiple agents, we randomly initiate (with random configurations) one of the four algorithms Lattimore & Szepesvári (2020): ε-greedy, Upper Confidence Bound (UCB) (Auer et al., 2002), Thompson sampling with random configurations (Thompson, 1933). Further, we have the option to randomly mix pooling techniques Ghosh et al. (2024) on top of any of the four algorithms.

A.2.3 Self-Masking-MNAR

Description: This pattern simulates a scenario where the probability of a value being missing is a direct function of the value itself. This pattern, commonly referred to as "self-masked MNAR ",

Table 4: Area Under the Curve (AUC) Performance on Categorical Columns with MCAR ($p = 0.4$) missingness.

OpenML Dataset	HyperImpute	MissForest	TabImpute	Mode
ChonicKidneyDisease	0.602	0.582	0.525	0.500
Dog Breeds Ranked	0.566	0.579	0.539	0.500
HappinessRank 2015	0.486	0.466	0.677	0.500
MY DB	0.480	0.514	0.521	0.500
Online Sales	0.790	0.809	0.869	0.500
Parkinson Dataset	0.665	0.640	0.523	0.500
acute-inflammations	0.761	0.756	0.723	0.500
aids	0.511	0.573	0.509	0.500
analcatdata creditscore	0.678	0.672	0.491	0.500
analcatdata cyyoung8092	0.683	0.649	0.611	0.500
analcatdata cyyoung9302	0.713	0.700	0.629	0.500
analcatdata impeach	0.751	0.749	0.706	0.500
analcatdata ncaa	0.549	0.547	0.500	0.500
analcatdata wildcat	0.749	0.682	0.674	0.500
auto price	0.749	0.802	0.761	0.500
backache	0.529	0.516	0.502	0.500
blogger	0.558	0.573	0.499	0.500
caesarian-section	0.534	0.499	0.518	0.500
cloud	0.436	0.409	0.440	0.500
cm1 req	0.677	0.658	0.602	0.500
cocomo numeric	0.629	0.618	0.655	0.500
conference attendance	0.500	0.512	0.499	0.500
corral	0.553	0.558	0.575	0.500
cpu	0.694	0.675	0.546	0.500
fl2000	0.608	0.468	0.533	0.500
flags	0.584	0.583	0.517	0.500
fruitfly	0.602	0.604	0.593	0.500
grub-damage	0.620	0.584	0.541	0.500
hutsof99 logis	0.569	0.568	0.583	0.500
iris	0.885	0.885	0.827	0.500
kidney	0.599	0.460	0.498	0.500
lowbwt	0.587	0.582	0.547	0.500
lung	0.558	0.483	0.496	0.500
lungcancer GSE31210	0.647	0.527	0.567	0.500
lymph	0.641	0.594	0.547	0.500
molecular-biology promoters	0.508	0.505	0.504	0.500
mux6	0.507	0.481	0.502	0.500
nadeem	0.594	0.521	0.542	0.500
nasa numeric	0.596	0.594	0.561	0.500
postoperative-patient-data	0.468	0.494	0.496	0.500
prnn crabs	0.840	0.687	0.737	0.500
prnn viruses	0.563	0.588	0.551	0.500
qualitative-bankruptcy	0.652	0.694	0.645	0.500
servo	0.528	0.516	0.480	0.500
sleuth case1202	0.544	0.590	0.521	0.500
sleuth case2002	0.609	0.564	0.526	0.500
sleuth ex2015	0.589	0.599	0.733	0.500
sleuth ex2016	0.562	0.588	0.532	0.500
tae	0.544	0.592	0.533	0.500
teachingAssistant	0.533	0.528	0.499	0.500
veteran	0.520	0.520	0.502	0.500
white-clover	0.626	0.598	0.622	0.500
zoo	0.754	0.710	0.764	0.500
Overall	0.609 ± 0.097	0.593 ± 0.097	0.577 ± 0.096	0.500 ± 0.000

is widely utilized in the missing-data literature to model unbalanced class problems (Mohan, 2018; Sportisse et al., 2020b). A classic example occurs in income surveys, where individuals at the extremes of the income distribution, both very high and very low earners, are often less likely to disclose their income (Moore & Welniak, 2000). Similar patterns appear in other domains, such as substance use reporting or medical contexts where patients with severe symptoms might be less able to complete follow-up assessments (Ibrahim & Molenberghs, 2009).

Within the structured missingness taxonomy proposed by (Jackson et al., 2023), this mechanism is classified as **MNAR-UP** (Unstructured, Probabilistic). It is "Unstructured" because the missingness of an entry (i, j) is conditionally independent of the missingness status of other entries, and "Probabilistic" as it is determined by a probability function rather than a deterministic rule.

Methodology: For each designated target column j, the probability of an entry (i, j) being missing is determined by a logistic function of its value. The relationship is defined as $\mathbb{P}(M_{ij} = 0|X^*_{ij}) = \sigma(\alpha \cdot X^*_{ij} + \beta_0)$ where $\sigma(z) = (1 + e^{-z})^{-1}$ is the sigmoid function.

Implementation Details: A random coefficient α is chosen from the set $\{-2, -1, 1, 2\}$ to introduce variability in the direction and magnitude of the value's effect on its missingness probability. The bias term β_0 is calibrated to achieve a target missingness proportion, p.

A.2.4 CENSORING-MNAR

Description: This pattern models missingness arising from the physical limitations of measurement instruments, where values falling below a lower Limit of Detection or above an upper Limit of Quantification are not recorded. This results in left-censored or right-censored data, a common obstacle in environmental science, epidemiology, and biomedical research (Helsel, 2011; Chen et al., 2013). In fields like metabolomics and proteomics, this type of missingness is explicitly recognized as left-censored MNAR (Karpievitch et al., 2009; Lazar et al., 2016), as the probability of being missing is directly determined by the concentration falling below the detection threshold. Failing to appropriately account for this, or using simplistic substitution methods like replacing with zero, can introduce substantial bias. Modeling `Censoring-MNAR` is therefore essential for evaluating imputation methods on datasets generated by instrumentation with inherent sensitivity constraints.

`Censoring-MNAR` maps to the **MNAR-UD** (Unstructured, Deterministic) category in the structured missingness framework. It is "Unstructured" as the missingness of an entry is independent of other missingness indicators, and "Deterministic" because any value falling beyond the censoring threshold is missing with certainty.

Methodology: For each column j, a censoring direction (left or right) is chosen with equal probability. A cutoff value is determined based on a specified quantile, q_{censor}, of the set of currently observed (non-missing) values in that column. Let $X^*_{:,j}$ denote the set of observed values in column j, i.e., $X^*_{:,j} = \{X_{ij} \mid M_{ij} = 1\}$.

- **Left-Censoring:** All values in column j that are less than the q_{censor}-th quantile of the observed values in that same column are set to missing. The threshold is a single scalar value calculated from the column's observed data.

$$M_{ij} = 0 \quad \text{if} \quad X_{ij} < \text{quantile}(X^*_{:,j}, q_{\text{censor}})$$

- **Right-Censoring:** All values in column j that are greater than the $(1 - q_{\text{censor}})$-th quantile of the observed values in that column are set to missing. The threshold is a single scalar value.

$$M_{ij} = 0 \quad \text{if} \quad X_{ij} > \text{quantile}(X^*_{:,j}, 1 - q_{\text{censor}})$$

Implementation Details: The choice between left- and right-censoring is made randomly for each column with a probability of 0.5 for each. We introduce a hyperparameter q_{censor} for the censoring quantile that controls the fraction of data to be censored from either tail of the distribution. For our evaluation, we use $q_{\text{censor}} = 0.25$.

A.2.5 PANEL-MNAR

Description: This pattern simulates participant attrition (dropout) in longitudinal and panel data studies. This creates missingness where the dropout of a subject at a specific time point means all subsequent data for that subject is unobserved. Attrition is an inherent feature of long-term studies, including clinical trials and cohort studies (Little & Rubin, 2019; Van Buuren, 2012). The primary concern is "attrition bias," which arises when dropout is systematic—meaning those who leave the study differ significantly from those who remain (Hausman & Wise, 1979). This often constitutes an MNAR mechanism, particularly in clinical settings where patients might withdraw due to adverse effects or perceived lack of treatment efficacy, directly linking the dropout to the (unobserved) future outcomes (Ibrahim & Molenberghs, 2009; Little, 1995).

Methodology: The columns of the data matrix X^* are assumed to represent ordered time points $t = 0, 1, ..., T-1$. For each subject (row) i, a random dropout time $t_{0,i}$ is sampled. All observations for that subject from time $t_{0,i}$ onwards are masked as missing.

$$M_{ij} = 0 \quad \forall j \geq t_{0,i}$$

Implementation Details: For each row i, the dropout time $t_{0,i}$ is sampled uniformly from the range of possible time steps, i.e., $t_{0,i} \sim \text{Unif}\{1, ..., T\}$.

A.2.6 POLARIZATION-MNAR

Description: This pattern simulates data where values falling in the middle of a feature's distribution are preferentially removed, simulating survey non-response from individuals with moderate opinions. This is implemented by setting values between the q-th and $(1-q)$-th quantiles to missing. A "soft" version makes the observation probability proportional to the value's distance from the median. `Polarization-MNAR` is recognized in the survey methodology literature as a form of voluntary response bias or self-selection bias (Bethlehem, 2010). One obvious example can be found in online product reviews, which frequently exhibit a U-shaped or J-shaped distribution, heavily skewed towards the highest and lowest ratings while the middle ground remains sparse—sometimes referred to as the "brag-and-moan" bias (Hu et al., 2009). Similarly, in political polling, nonresponse bias can be exacerbated if highly polarized individuals are more motivated to participate than moderates, potentially exaggerating measures of mass polarization Cavari & Freedman (2023).

This pattern maps to the "Unstructured" MNAR categories of (Jackson et al., 2023). Specifically, our hard polarization variant, where values within a quantile range are missing with certainty, is an instance of **MNAR-UD** (Unstructured, Deterministic). Our soft polarization variant, where the missingness probability is a function of the value's distance from the median, is an example of **MNAR-UP** (Unstructured, Probabilistic).

Hard Polarization Methodology: For each column j, values falling between two quantiles are deterministically masked. The quantiles are calculated using only the set of currently observed (non-'NaN') values in that column. Let $X^*_{:,j}$ denote this set of observed values, i.e., $X^*_{:,j} = \{X_{ij} \mid M_{ij} = 1\}$. The lower and upper thresholds, L_j and H_j, are defined as:

$$L_j = \text{quantile}(X^*_{:,j}, q_{\text{thresh}})$$

$$H_j = \text{quantile}(X^*_{:,j}, 1 - q_{\text{thresh}})$$

An entry X_{ij} is then masked if its value falls between these two scalar thresholds:

$$M_{ij} = 0 \quad \text{if} \quad L_j < X_{ij} < H_j$$

Soft Polarization Methodology: The probability of a value being observed is made proportional to its normalized absolute distance from the column's median, μ_j. This creates a softer, probabilistic version of the polarization effect. The missing probability is given by:

$$\mathbb{P}(M_{ij} = 0) = \epsilon + (1 - 2\epsilon)\frac{|X^*_{ij} - \mu_j|^\alpha}{\max_k(|X^*_{kj} - \mu_j|^\alpha)}$$

Implementation Details: For the hard polarization pattern, we introduce a hyperparameter q_{thresh} for the threshold quantile that defines the central portion of the distribution to be masked. For the soft polarization pattern, we have an exponent parameter α that controls the intensity of the polarization effect. Higher values of α make the observation probability more sensitive to deviations from the median. In the soft version, we also have a baseline probability ϵ that ensures even values at the median have a non-zero chance of being observed.

A.2.7 LATENT-FACTOR-MNAR

Description: This pattern generates a complex missingness structure where the probability of an entry being missing depends on unobserved (latent) characteristics of both its row and its column. This is most common in recommender systems and collaborative filtering, where the data (e.g., user ratings) are inherently MNAR (Marlin & Zemel, 2009; Steck, 2010). Users do not select items to rate uniformly; rather, their exposure to items and their decisions to provide a rating are strongly influenced by their underlying (latent) preferences-the very values the system aims to predict (Schnabel et al., 2016). This creates a selection bias where observed ratings are a biased sample of the full data. A standard approach in the literature assumes a low-rank structure for both the underlying data matrix and the missingness mechanism (propensity score matrix), implying they are governed by a shared set of latent factor (Sportisse et al., 2020a; Jin et al., 2022). Recent work in causal matrix completion explicitly models these latent confounders (Agarwal et al., 2023).

Methodology: The probability of an entry (i, j) being observed is modeled using a low-rank bilinear model. The observation probability is given by the sigmoid of a dot product of latent factors plus bias terms:

$$\mathbb{P}(M_{ij} = 1) = \sigma(u_i^T v_j + b_i + c_j)$$

where $u_i \in \mathbb{R}^k$ and $v_j \in \mathbb{R}^k$ are k-dimensional latent vectors for row i and column j, and b_i and c_j are scalar biases for the row and column, respectively.

Implementation Details: We specify the rank k that defines the dimensionality of the latent space, sampled as an integer. The elements of the latent factor matrices $U \in \mathbb{R}^{N\times k}$ and $V \in \mathbb{R}^{D\times k}$, and the bias vectors $b \in \mathbb{R}^N$ and $c \in \mathbb{R}^D$, are sampled independently from a standard normal distributions.

A.2.8 CLUSTER-MNAR

Description: This pattern induces missingness based on latent group-level characteristics. Rows and columns are first assigned to discrete clusters, and each cluster has a random effect that uniformly influences the observation probability of all its members. Such structures are prevalent in education (students clustered in schools), healthcare (patients clustered in hospitals), and cross-national surveys. In these settings, missing data patterns are often not independent across observations but rather clustered (Van Buuren, 2011). For example, in multi-center clinical trials or Cluster Randomized Trials, missingness can be heavily influenced by site-specific factors such as resource availability or staff training (Diaz-Ordaz et al., 2014). Ignoring this hierarchical structure during imputation fails to account for the within-cluster correlation and can lead to biased estimates (Enders et al., 2016). Because the missingness mechanis is related to these cluster-level effects, which may themselves be latent, the data is MNAR.

In the structured missigness taxonomy, we classify Cluster-MNAR as **MNAR-UP** (Unstructured, Probabilistic) due to the the probabilistic dependence on unobserved factors, without dependence on other missingness indicators.

Methodology: The probability of an entry (i, j) being observed is determined by an additive model of random effects corresponding to the cluster assignments of its row i and column j. Denoting the row assignments by $C_R(i)$ and column assignments by $C_C(j)$, the observation probability is modeled as:

$$\mathbb{P}(M_{ij} = 1) = \sigma(g_{C_R(i)} + h_{C_C(j)} + \epsilon_{ij})$$

where:

- $\sigma(z) = (1 + e^{-z})^{-1}$ is the sigmoid function.

- $g_k \sim \mathcal{N}(0, \tau_r^2)$ is the random effect for row cluster k.
- $h_l \sim \mathcal{N}(0, \tau_c^2)$ is the random effect for column cluster l.
- $\epsilon_{ij} \sim \mathcal{N}(0, \epsilon_{\text{std}}^2)$ is an entry-specific noise term.

Implementation Details: For a matrix with N and D columns, row assignments $C_R(i)$ are draw uniformly from $\{0, ..., K_R - 1\}$ and column assignments $C_C(j)$ are drawn uniformly from $\{0, ..., K_C - 1\}$, where K_R and K_C are the total number of row and column clusters, respectively. The number of row clusters K_R, the number of column clusters K_C, and the standard deviation of the random effects (τ_r, τ_c, ϵ_{std}) are hyperparameters specified for the data generation process.

A.2.9 TWO-PHASE-MNAR

Description: This pattern mimics multi-stage data collection, mirroring established methodologies such as "two-phase sampling" (or "double sampling") (Neyman, 1938) and "Planned Missing Data Designs" (Graham et al., 2006). These designs are frequently employed in large-scale surveys and epidemiological studies to manage costs and participant burden when certain variables are expensive or difficult to measure (Rhemtulla & Hancock, 2016). Another example includes market research where basic demographics are collected from all participants, but detailed purchasing behavior is only gathered from a subset, with missingness related to income level. In these designs, a full sample provides baseline information ("cheap" features), and a subset is strategically selected for follow-up ("expensive" features).

Methodology: Let $\mathcal{F} = \{0, 1, ..., D - 1\}$ be the set of all column indices in the data matrix X. This set is randomly partitioned into a "cheap" subset $\mathcal{C} \subset \mathcal{F}$ and an "expensive" subset $\mathcal{E} \subset \mathcal{F}$, such that $\mathcal{C} \cup \mathcal{E} = \mathcal{F}$ and $\mathcal{C} \cap \mathcal{E} = \emptyset$. By design, features in the cheap set $\mathcal{C}$ are always observed.

The decision to collect the expensive features for a given row i is based on a logistic model applied to its cheap features. Let $X_{i,\mathcal{C}}$ denote the vector of values $\{X_{ij} \mid j \in \mathcal{C}\}$ for row i. A score is calculated for each row:

$$s_i = \text{normalize}(X_{i,\mathcal{C}}^T w)$$

where w is a vector of random weights and the 'normalize' function applies z-score normalization to the resulting scores across all rows.

The probability that all expensive features are observed for row i is then given by:

$$\mathbb{P}(M_{ij} = 1 \text{ for all } j \in \mathcal{E}) = \sigma(\alpha + \beta \cdot s_i)$$

If the expensive features for row i are not observed (based on the probability above), then all of its values in the expensive columns are masked as missing, i.e., $M_{ij} = 1$ for all $j \in \mathcal{E}$.

Implementation Details: A fraction of columns, e.g., 50%, are randomly assigned to be "cheap". The weight vector for the scoring model is sampled from a standard normal distribution, $w \sim \mathcal{N}(0, 1)$. Parameters α, β control the base rate and score-dependency of the observation probability. In our implementation, they are set to default values of $\alpha = 0$ and $\beta = 2.0$.

A.3 ADDITIONAL TABLES

Table 5: Other imputation methods

Name	Description
Column-wise mean (Hawthorne & Elliott, 2005)	Mean of columns
SoftImpute (Hastie et al., 2015)	Iterative soft thresholding singular value decomposition based on a low-rank assumption on the data
k-Nearest Neighbors (Fix & Hodges, 1989)	Row-wise nearest neighbors mean
HyperImpute (Jarrett et al., 2022)	Iterative imputation method optimizing over a suite of imputation methods
Optimal transport method (Muzellec et al., 2020)	Uses optimal transport distances as a loss to impute missing values based on the principle that two randomly drawn batches from the same dataset should share similar data distributions
MissForest (Stekhoven & Bühlmann, 2011)	Repeatedly trains a random forest model for each variable on the observed values to predict and fill in missing entries until convergence
ICE (van Buuren & Groothuis-Oudshoorn, 2011)	Imputation with iterative and chained equations of linear/logistic models for conditional expectations
MICE (Royston & White, 2011)	Handles missing data by iteratively imputing each incomplete variable using regression models that condition on all other variables
GAIN (Yoon et al., 2018)	Adapts generative adversarial networks (Goodfellow et al., 2020) where the generator imputes missing values and the discriminator identifies which components are observed versus imputed
MIWAE (Mattei & Frellsen, 2019)	Learns a deep latent variable model and then performs importance sampling for imputation
ForestDiffusion (Jolicoeur-Martineau et al., 2024)	Trains a diffusion model using XGBoost directly on incomplete tabular data and then fills in missing values with an adapted inpainting algorithm
TabPFN	The `tabpfn-extensions` package includes a part to impute missing entries in a table column-by-column using TabPFN.

Table 6: Imputation Accuracy ± Standard Error by Missingness Pattern (All Methods)

Pattern	TabImpute	EWF-TabPFN	HyperImpute	OT	MissForest
MCAR	0.882 ± 0.021	0.817 ± 0.024	0.804 ± 0.031	0.855 ± 0.019	0.867 ± 0.022
NN-MNAR	0.900 ± 0.019	0.876 ± 0.020	0.760 ± 0.036	0.814 ± 0.021	0.818 ± 0.029
Self-Masking-MNAR	0.703 ± 0.038	0.682 ± 0.042	0.689 ± 0.039	0.568 ± 0.037	0.638 ± 0.040
Col-MAR	0.877 ± 0.030	0.855 ± 0.027	0.814 ± 0.040	0.750 ± 0.040	0.773 ± 0.039
Block-MNAR	0.890 ± 0.026	0.905 ± 0.026	0.873 ± 0.027	0.857 ± 0.024	0.860 ± 0.023
Seq-MNAR	0.920 ± 0.014	0.905 ± 0.015	0.864 ± 0.030	0.894 ± 0.014	0.829 ± 0.031
Panel-MNAR	0.915 ± 0.025	0.711 ± 0.048	0.865 ± 0.033	0.887 ± 0.025	0.912 ± 0.020
Polarization-MNAR	0.804 ± 0.024	0.879 ± 0.021	0.622 ± 0.039	0.802 ± 0.020	0.567 ± 0.033
Soft-Polarization-MNAR	0.759 ± 0.045	0.864 ± 0.024	0.711 ± 0.034	0.750 ± 0.029	0.667 ± 0.041
Latent-Factor-MNAR	0.891 ± 0.021	0.883 ± 0.018	0.775 ± 0.036	0.842 ± 0.026	0.834 ± 0.023
Cluster-MNAR	0.903 ± 0.014	0.871 ± 0.021	0.839 ± 0.028	0.828 ± 0.022	0.830 ± 0.021
Two-Phase-MNAR	0.886 ± 0.026	0.851 ± 0.029	0.865 ± 0.031	0.807 ± 0.028	0.873 ± 0.020
Censoring-MNAR	0.710 ± 0.032	0.593 ± 0.045	0.786 ± 0.041	0.589 ± 0.036	0.671 ± 0.038
Overall	0.849 ± 0.008	0.823 ± 0.009	0.790 ± 0.010	0.788 ± 0.009	0.780 ± 0.009

Pattern	K-Nearest Neighbors	ICE	SoftImpute	Col Mean	DiffPuter
MCAR	0.750 ± 0.025	0.659 ± 0.041	0.617 ± 0.044	0.478 ± 0.041	0.478 ± 0.041
NN-MNAR	0.741 ± 0.026	0.627 ± 0.039	0.679 ± 0.035	0.497 ± 0.041	0.497 ± 0.041
Self-Masking-MNAR	0.614 ± 0.038	0.673 ± 0.049	0.396 ± 0.044	0.293 ± 0.038	0.293 ± 0.038
Col-MAR	0.839 ± 0.028	0.825 ± 0.038	0.703 ± 0.040	0.622 ± 0.046	0.598 ± 0.047
Block-MNAR	0.860 ± 0.028	0.812 ± 0.037	0.799 ± 0.042	0.782 ± 0.034	0.806 ± 0.029
Seq-MNAR	0.885 ± 0.018	0.815 ± 0.037	0.783 ± 0.036	0.775 ± 0.033	0.775 ± 0.033
Panel-MNAR	0.899 ± 0.028	0.797 ± 0.044	0.340 ± 0.053	0.787 ± 0.037	0.811 ± 0.032
Polarization-MNAR	0.641 ± 0.028	0.560 ± 0.041	0.665 ± 0.048	0.964 ± 0.012	0.964 ± 0.012
Soft-Polarization-MNAR	0.580 ± 0.042	0.729 ± 0.031	0.677 ± 0.033	0.747 ± 0.030	0.747 ± 0.030
Latent-Factor-MNAR	0.764 ± 0.029	0.703 ± 0.042	0.714 ± 0.039	0.590 ± 0.045	0.590 ± 0.045
Cluster-MNAR	0.774 ± 0.024	0.750 ± 0.042	0.627 ± 0.046	0.558 ± 0.044	0.558 ± 0.044
Two-Phase-MNAR	0.898 ± 0.020	0.876 ± 0.032	0.678 ± 0.047	0.671 ± 0.042	0.671 ± 0.042
Censoring-MNAR	0.515 ± 0.047	0.866 ± 0.035	0.455 ± 0.054	0.346 ± 0.040	0.307 ± 0.037
Overall	0.751 ± 0.010	0.746 ± 0.011	0.626 ± 0.013	0.624 ± 0.013	0.623 ± 0.013

Pattern	TabPFN	MICE	MIWAE	GAIN
MCAR	0.415 ± 0.041	0.329 ± 0.044	0.254 ± 0.043	0.545 ± 0.039
NN-MNAR	0.428 ± 0.041	0.300 ± 0.049	0.230 ± 0.043	0.392 ± 0.049
Self-Masking-MNAR	0.268 ± 0.037	0.611 ± 0.051	0.217 ± 0.041	0.452 ± 0.056
Col-MAR	0.549 ± 0.050	0.520 ± 0.054	0.488 ± 0.048	0.275 ± 0.054
Block-MNAR	0.582 ± 0.051	0.502 ± 0.048	0.606 ± 0.039	0.202 ± 0.051
Seq-MNAR	0.638 ± 0.045	0.475 ± 0.050	0.584 ± 0.045	0.204 ± 0.048
Panel-MNAR	0.234 ± 0.042	0.553 ± 0.048	0.269 ± 0.045	0.536 ± 0.059
Polarization-MNAR	0.907 ± 0.029	0.192 ± 0.037	0.562 ± 0.027	0.294 ± 0.045
Soft-Polarization-MNAR	0.600 ± 0.050	0.219 ± 0.038	0.548 ± 0.036	0.425 ± 0.062
Latent-Factor-MNAR	0.499 ± 0.048	0.338 ± 0.047	0.355 ± 0.045	0.296 ± 0.046
Cluster-MNAR	0.499 ± 0.047	0.327 ± 0.044	0.330 ± 0.044	0.357 ± 0.048
Two-Phase-MNAR	0.478 ± 0.049	0.564 ± 0.048	0.529 ± 0.049	0.228 ± 0.049
Censoring-MNAR	0.342 ± 0.041	0.648 ± 0.050	0.308 ± 0.045	0.320 ± 0.051
Overall	0.495 ± 0.014	0.429 ± 0.014	0.407 ± 0.013	0.348 ± 0.015

Table 7: Mean Column-wise R^2 ± Standard Error by Missingness Pattern

Pattern	EWF-TabPFN	TabImpute	HyperImpute	ICE	MissForest
MCAR	0.395 ± 0.036	**0.414 ± 0.035**	0.409 ± 0.035	0.387 ± 0.035	0.401 ± 0.036
NN-MNAR	**0.387 ± 0.035**	0.382 ± 0.034	0.364 ± 0.034	0.348 ± 0.033	0.351 ± 0.033
Self-Masking-MNAR	**0.297 ± 0.039**	0.285 ± 0.039	0.234 ± 0.038	0.250 ± 0.037	0.207 ± 0.030
Col-MAR	**0.308 ± 0.033**	0.289 ± 0.035	0.285 ± 0.034	0.287 ± 0.034	0.242 ± 0.032
Block-MNAR	**0.283 ± 0.032**	0.256 ± 0.033	0.242 ± 0.034	0.229 ± 0.033	0.221 ± 0.033
Seq-MNAR	0.234 ± 0.030	0.218 ± 0.027	**0.246 ± 0.029**	0.234 ± 0.030	0.210 ± 0.028
Panel-MNAR	0.275 ± 0.028	**0.290 ± 0.029**	0.285 ± 0.027	0.271 ± 0.029	0.271 ± 0.028
Polarization-MNAR	**0.230 ± 0.022**	0.190 ± 0.019	0.189 ± 0.020	0.177 ± 0.021	0.156 ± 0.017
Soft-Polarization-MNAR	**0.177 ± 0.027**	0.148 ± 0.024	0.146 ± 0.024	0.137 ± 0.023	0.131 ± 0.022
Latent-Factor-MNAR	**0.347 ± 0.034**	0.338 ± 0.033	0.335 ± 0.034	0.331 ± 0.033	0.322 ± 0.034
Cluster-MNAR	**0.350 ± 0.036**	0.342 ± 0.035	0.342 ± 0.037	0.325 ± 0.036	0.325 ± 0.036
Two-Phase-MNAR	**0.370 ± 0.035**	0.331 ± 0.037	0.333 ± 0.037	0.334 ± 0.036	0.310 ± 0.034
Censoring-MNAR	**0.177 ± 0.025**	0.143 ± 0.020	0.121 ± 0.019	0.125 ± 0.019	0.097 ± 0.017
Overall	**0.295 ± 0.009**	0.279 ± 0.009	0.272 ± 0.009	0.264 ± 0.009	0.249 ± 0.009

Pattern	OT	K-Nearest Neighbors	MICE	GAIN	SoftImpute
MCAR	**0.401 ± 0.034**	0.323 ± 0.036	0.302 ± 0.036	0.318 ± 0.031	0.265 ± 0.041
NN-MNAR	**0.334 ± 0.033**	0.278 ± 0.031	0.254 ± 0.033	0.265 ± 0.026	0.223 ± 0.043
Self-Masking-MNAR	0.211 ± 0.034	0.207 ± 0.033	**0.264 ± 0.044**	0.224 ± 0.029	0.166 ± 0.030
Col-MAR	0.221 ± 0.031	**0.227 ± 0.032**	0.182 ± 0.030	0.156 ± 0.027	0.167 ± 0.033
Block-MNAR	**0.199 ± 0.029**	0.186 ± 0.029	0.155 ± 0.027	0.098 ± 0.016	0.165 ± 0.035
Seq-MNAR	0.192 ± 0.023	**0.213 ± 0.027**	0.139 ± 0.023	0.099 ± 0.015	0.181 ± 0.032
Panel-MNAR	0.247 ± 0.025	**0.277 ± 0.028**	0.146 ± 0.021	0.167 ± 0.023	0.181 ± 0.032
Polarization-MNAR	**0.177 ± 0.018**	0.146 ± 0.018	0.109 ± 0.015	0.109 ± 0.013	0.118 ± 0.021
Soft-Polarization-MNAR	**0.108 ± 0.020**	0.075 ± 0.018	0.066 ± 0.016	0.078 ± 0.014	0.077 ± 0.021
Latent-Factor-MNAR	**0.306 ± 0.031**	0.246 ± 0.031	0.227 ± 0.032	0.202 ± 0.023	0.194 ± 0.039
Cluster-MNAR	**0.314 ± 0.033**	0.254 ± 0.032	0.225 ± 0.032	0.239 ± 0.029	0.187 ± 0.038
Two-Phase-MNAR	0.260 ± 0.030	**0.293 ± 0.031**	0.191 ± 0.030	0.198 ± 0.026	0.190 ± 0.035
Censoring-MNAR	0.084 ± 0.016	0.095 ± 0.011	**0.131 ± 0.022**	0.127 ± 0.020	0.081 ± 0.021
Overall	**0.235 ± 0.009**	0.217 ± 0.008	0.184 ± 0.008	0.175 ± 0.007	0.169 ± 0.009

Pattern	ForestDiffusion	TabPFN	MIWAE	Col Mean
MCAR	**0.220 ± 0.029**	0.070 ± 0.008	0.036 ± 0.005	0.000 ± 0.000
NN-MNAR	**0.177 ± 0.026**	0.042 ± 0.006	0.025 ± 0.003	0.000 ± 0.000
Self-Masking-MNAR	**0.116 ± 0.024**	0.106 ± 0.016	0.026 ± 0.004	0.000 ± 0.000
Col-MAR	**0.108 ± 0.020**	0.081 ± 0.011	0.030 ± 0.003	0.000 ± 0.000
Block-MNAR	**0.106 ± 0.017**	0.051 ± 0.008	0.023 ± 0.003	0.000 ± 0.000
Seq-MNAR	**0.089 ± 0.014**	0.034 ± 0.003	0.022 ± 0.003	0.000 ± 0.000
Panel-MNAR	**0.120 ± 0.016**	0.083 ± 0.011	0.039 ± 0.006	0.000 ± 0.000
Polarization-MNAR	**0.091 ± 0.012**	0.036 ± 0.004	0.029 ± 0.004	0.000 ± 0.000
Soft-Polarization-MNAR	**0.031 ± 0.004**	0.004 ± 0.001	0.014 ± 0.001	0.000 ± 0.000
Latent-Factor-MNAR	**0.152 ± 0.022**	0.053 ± 0.007	0.028 ± 0.003	0.000 ± 0.000
Cluster-MNAR	**0.181 ± 0.027**	0.058 ± 0.009	0.033 ± 0.005	0.000 ± 0.000
Two-Phase-MNAR	**0.126 ± 0.022**	0.086 ± 0.012	0.022 ± 0.003	0.000 ± 0.000
Censoring-MNAR	0.071 ± 0.011	**0.072 ± 0.018**	0.067 ± 0.018	0.000 ± 0.000
Overall	**0.122 ± 0.006**	0.060 ± 0.003	0.030 ± 0.002	0.000 ± 0.000

Table 8: Mean Normalized Negative RMSE ± Standard Error by Missingness Pattern. Note that these normalized values are slightly different than Tab. 1 because the nonlinear model is included here.

Pattern	TabImpute	HyperImpute	TabImpute$_{\text{Nonlinear}}$	MissForest
MCAR	**0.880 ± 0.021**	0.803 ± 0.031	0.835 ± 0.022	0.866 ± 0.022
NN-MNAR	**0.898 ± 0.019**	0.758 ± 0.036	0.835 ± 0.022	0.816 ± 0.029
Self-Masking-MNAR	**0.705 ± 0.037**	0.689 ± 0.039	0.613 ± 0.043	0.639 ± 0.041
Col-MAR	**0.868 ± 0.030**	0.806 ± 0.040	0.836 ± 0.029	0.764 ± 0.038
Block-MNAR	**0.890 ± 0.026**	0.873 ± 0.027	0.868 ± 0.029	0.860 ± 0.023
Seq-MNAR	**0.919 ± 0.015**	0.863 ± 0.030	0.890 ± 0.018	0.828 ± 0.031
Panel-MNAR	**0.893 ± 0.027**	0.847 ± 0.034	0.448 ± 0.063	0.891 ± 0.022
Polarization-MNAR	**0.800 ± 0.024**	0.619 ± 0.039	0.751 ± 0.030	0.564 ± 0.032
Soft-Polarization-MNAR	0.756 ± 0.045	0.709 ± 0.034	**0.808 ± 0.034**	0.665 ± 0.041
Latent-Factor-MNAR	**0.888 ± 0.020**	0.773 ± 0.035	0.857 ± 0.020	0.832 ± 0.024
Cluster-MNAR	**0.896 ± 0.016**	0.833 ± 0.029	0.858 ± 0.017	0.824 ± 0.022
Two-Phase-MNAR	**0.879 ± 0.026**	0.859 ± 0.031	0.871 ± 0.026	0.867 ± 0.020
Censoring-MNAR	0.711 ± 0.032	**0.790 ± 0.039**	0.623 ± 0.039	0.673 ± 0.036
Overall	**0.845 ± 0.008**	0.786 ± 0.010	0.776 ± 0.010	0.776 ± 0.009

Table 9: Synthetic Data Generation Parameters

Missingness Pattern	**Parameter Name**	**Symbol**	**Value**
MCAR	Missing probability	p	0.4
Col-MAR	Missing probability	p	0.4
NN-MNAR	Neighborhood size	$\lvert N_{ij}\rvert$	Variable
	Network layers	L	Random
	Network depth	d	Random
	Weight initialization	W	Random
	Bias initialization	b	Random
Self-Masking-MNAR	Coefficient set	α	$\{-2,-1,1,2\}$
	Target missing proportion	$p_{missing}$	Variable
Block-MNAR	Missing probability	p	0.4
	Matrix size N	N	100
	Matrix size T	T	50
	Row blocks	B_r	10
	Column blocks	B_c	10
	Convolution type	-	mean
Seq-MNAR	Missing probability	p	0.4
	Algorithm	-	epsilon_greedy
	Pooling	-	False
	Epsilon	ϵ	0.4
	Epsilon decay	γ	0.99
	Random seed	s	42
Panel-MNAR	No explicit hyperparameters (dropout time sampled uniformly)		
Polarization-MNAR	Threshold quantile	q_{thresh}	0.25
Soft-Polarization-MNAR	Polarization alpha	α	2.5
	Polarization epsilon	ϵ	0.05
Latent-Factor-MNAR	Latent rank (low)	k_{low}	1
	Latent rank (high)	k_{high}	5
Cluster-MNAR	Number of row clusters	K_R	5
	Number of column clusters	K_C	4
Two-Phase-MNAR	Cheap feature fraction	f_{cheap}	0.4
Censoring-MNAR	Censoring quantile	q_{censor}	0.25

Table 10: OpenML datasets

Dataset	Size	Domain	Description
EgyptianSkulls	150×5	Anthropology	Cranial measurements over time in Egypt
humans_numeric	75×15	Biology	Human body measurements
FacultySalaries	50×5	Education/Economics	University faculty salary data
SMSA	59×16	Demographics/Economics	U.S. metropolitan statistical area data
Student-Scores	56×13	Education	Student exam scores
analcatdata_election2000	67×15	Political science	2000 U.S. presidential election results
analcatdata_gviolence	74×9	Criminology	Gun violence statistics
analcatdata_olympic2000	66×12	Sports/Economics	Olympic results and country stats
baskball	96×5	Sports analytics	Basketball performance data
visualizing_hamster	73×6	Education/Toy	Example dataset for teaching
witmer_census_1980	50×5	Demographics	U.S. census microdata (1980)
MercuryinBass	53×10	Environmental chemistry	Mercury concentrations in fish
SolarPower	204×5	Energy/Engineering	Solar power output records
WineDataset	178×14	Chemistry/Oenology	Wine physicochemical properties
alcohol-qcm-sensor	125×15	Analytical chemistry	Alcohol detection sensor readings
benzo32	195×33	Chemistry/Toxicology	Benzodiazepine compound data
machine_cpu	209×7	Computer systems	Predicting CPU performance
pwLinear	200×11	Mathematics/Engineering	Piecewise linear regression benchmark
pyrim	74×28	Chemistry/Pharmacology	Pyrimethamine bioassay compounds
slump	103×10	Civil engineering	Concrete slump test properties
ICU	200×20	Medicine	Intensive care patient data
appendicitis_test	106×8	Medicine	Appendicitis diagnosis
appendicitis_test_edsa	106×8	Medicine	Educational appendicitis dataset
breast-cancer-coimbra	116×10	Medicine	Breast cancer diagnosis data
Rainfall-in-Kerala-1901-2017	117×18	Climate science	Rainfall time series in Kerala
pollution	60×16	Environmental science	Air pollution measurements
treepipit	86×10	Ecology	Bird habitat distribution
autoPrice	159×16	Business/Economics	Automobile pricing dataset
dataset_analcatdata_creditscore	100×7	Finance	Credit scoring dataset
Swiss-banknote-conterfeit-detection	200×7	Finance/Fraud	Banknote authenticity classification
Glass-Classification	214×10	Forensics/Materials	Glass chemical composition (forensics)
chatfield_4	235×13	Statistics/Time series	Textbook time series data (Chatfield)
chscase_vine1	52×10	Agriculture/Statistics	Vine growth study
edm	154×18	Education	Student learning performance
metafeatures	75×32	Meta-learning	Dataset-level features
rabe_131	50×6	Chemistry/Benchmark	Spectroscopy regression dataset
rabe_148	66×6	Chemistry/Benchmark	Spectroscopy regression dataset
rabe_265	51×7	Chemistry/Benchmark	Spectroscopy regression dataset
sleuth_case1201	50×7	Statistics/Education	Applied regression textbook data
sleuth_ex1605	62×6	Statistics/Education	Applied regression textbook data
wisconsin	194×33	Medicine	Wisconsin breast cancer dataset

Table 11: Non-normalized RMSE values for MCAR pattern by dataset. Dataset columns are standardized based on observed values (mean 0, variance 1).

Dataset	TabImpute	EWF-TabPFN	HyperImpute	MissForest
EgyptianSkulls	**0.901**	0.917	0.961	0.946
FacultySalaries	0.607	0.693	0.811	**0.567**
Glass-Classification	0.889	0.937	**0.810**	0.886
ICU	1.059	**1.045**	1.137	1.112
MercuryinBass	**1.311**	1.373	1.377	1.343
Rainfall-in-Kerala-1901-2017	0.908	0.944	**0.902**	0.950
SMSA	0.840	0.814	0.939	**0.786**
SolarPower	0.889	**0.805**	0.873	0.888
Student-Scores	0.429	**0.392**	0.441	0.435
Swiss-banknote-conterfeit-detection	0.774	0.976	0.856	**0.730**
WineDataset	0.829	0.928	0.803	**0.797**
alcohol-qcm-sensor	**0.467**	0.590	0.580	0.517
analcatdata_election2000	**0.364**	0.538	0.662	0.615
analcatdata_gviolence	**0.687**	0.796	0.801	0.877
analcatdata_olympic2000	1.950	**1.871**	1.922	1.895
appendicitis_test	0.694	0.861	**0.650**	0.792
appendicitis_test_edsa	0.534	0.668	**0.532**	0.569
autoPrice	0.735	0.834	0.762	**0.702**
baskball	**1.008**	1.028	1.100	1.109
benzo32	1.070	1.055	1.055	**1.053**
breast-cancer-coimbra	1.068	**1.058**	1.183	1.098
chatfield_4	**0.473**	0.476	0.531	0.492
chscase_vine1	0.928	**0.809**	0.996	0.833
dataset_analcatdata_creditscore	1.238	**1.063**	1.131	1.122
divorce_prediction	0.542	0.525	0.528	**0.467**
edm	0.612	0.763	**0.553**	0.566
humans_numeric	0.989	**0.952**	0.970	0.991
machine_cpu	0.902	1.039	0.956	**0.858**
metafeatures	2.609	2.263	**2.090**	2.225
pollution	1.946	1.967	2.065	**1.837**
pwLinear	**1.031**	1.075	1.356	1.356
pyrim	**0.847**	0.877	0.863	0.859
rabe_131	1.016	**0.792**	1.003	1.031
rabe_148	**0.905**	0.985	1.017	0.958
rabe_265	1.104	1.131	1.298	**1.090**
sleuth_case1201	0.940	1.054	**0.939**	0.963
sleuth_ex1605	**1.026**	1.087	1.257	1.071
slump	0.750	0.871	**0.650**	0.805
treepipit	1.226	1.265	**1.169**	1.172
visualizing_hamster	0.754	0.872	0.905	**0.750**
wisconsin	0.854	0.777	**0.685**	0.783
witmer_census_1980	0.654	0.704	**0.616**	0.637

Table 12: Non-normalized RMSE Values for MCAR Pattern by Dataset including ReMasker. Note that we could not replicate ReMasker's results using their open-source implementation. In order to not misrepresent their method, we do not include this table in our main results.

Dataset	TabImpute	HyperImpute	MissForest	ReMasker
EgyptianSkulls	**0.901**	0.961	0.946	2.329
FacultySalaries	0.607	0.811	**0.567**	1.534
Glass-Classification	0.889	**0.810**	0.886	3.126
ICU	**1.059**	1.137	1.112	1.479
MercuryinBass	**1.311**	1.377	1.343	2.198
Rainfall-in-Kerala-1901-2017	0.908	**0.902**	0.950	3.560
SMSA	0.840	0.939	**0.786**	1.979
SolarPower	0.889	**0.873**	0.888	1.589
Student-Scores	**0.429**	0.441	0.435	1.785
Swiss-banknote-conterfeit-detection	0.774	0.856	**0.730**	1.364
WineDataset	0.829	0.803	**0.797**	1.454
alcohol-qcm-sensor	**0.467**	0.580	0.517	2.044
analcatdata_election2000	**0.364**	0.662	0.615	4.563
analcatdata_gviolence	**0.687**	0.801	0.877	1.617
analcatdata_olympic2000	1.950	1.922	**1.895**	2.787
appendicitis_test	0.694	**0.650**	0.792	2.174
appendicitis_test_edsa	0.534	**0.532**	0.569	1.986
autoPrice	0.735	0.762	**0.702**	2.190
baskball	**1.008**	1.100	1.109	2.246
benzo32	1.070	1.055	**1.053**	3.282
breast-cancer-coimbra	**1.068**	1.183	1.098	1.820
chatfield_4	**0.473**	0.531	0.492	3.545
chscase_vine1	0.928	0.996	**0.833**	2.720
dataset_analcatdata_creditscore	1.238	1.131	**1.122**	1.469
divorce_prediction	0.542	0.528	**0.467**	1.216
edm	0.612	**0.553**	0.566	1.415
humans_numeric	0.989	**0.970**	0.991	4.165
machine_cpu	0.902	0.956	**0.858**	1.402
metafeatures	2.609	**2.090**	2.225	2.715
pollution	1.946	2.065	**1.837**	2.985
pwLinear	**1.031**	1.356	1.356	1.040
pyrim	**0.847**	0.863	0.859	1.647
rabe_131	1.016	**1.003**	1.031	2.076
rabe_148	**0.905**	1.017	0.958	2.508
rabe_265	1.104	1.298	**1.090**	2.633
sleuth_case1201	0.940	**0.939**	0.963	2.455
sleuth_ex1605	**1.026**	1.257	1.071	2.327
slump	0.750	**0.650**	0.805	1.960
treepipit	1.226	**1.169**	1.172	1.648
visualizing_hamster	0.754	0.905	**0.750**	1.884
wisconsin	0.854	**0.685**	0.783	2.422
witmer_census_1980	0.654	**0.616**	0.637	2.487